City of Homer
www.cityofhomer-ak.gov

Office of the City Manager
491 East Pioneer Avenue
Homer, Alaska 99603
citymanager@cityofhomer-ak.gov
(p) 907-235-8121 x2222
(f) 907-235-3148

Memorandum

TO: Mayor Lord and Homer City Council

FROM: Melissa Jacobsen, City Manager

DATE: January 8, 2025

SUBJECT: City Manager's Report for January 13, 2025 Council Meeting

Surplus Sale

Sealed bids for City surplus equipment are being accepted through Wednesday, January 22. For full details visit, www.cityofhomer-ak.gov/cityclerk/city-homer-surplusequipment-sale-winter-2025 . Looking ahead to future surplus sales I've asked the City Clerk to research some online auction platforms, such as Ritchie Brothers and Alaska Premier Auctions where the City can upload the information and the auction company facilitates the online bidding and collection of payment. My understanding is the auction company retains a portion of the sales and submits the balance to the City. For the amount of staff time for the Clerk's office to manage these surplus sales, we may find a savings. This also has the potential to expand our pool of bidders. More to come!

Digitization of the *Homer News* Completed

In late October the Library shipped the entire collection of the *Homer News* on microfilm to Ancestry.com, who spent a couple months scanning and indexing the materials. The archive from 1954 to 2021 is now available online. It can be accessed from any computer in the Library or a personal subscription to Newpapers.com.

Library Author Talk and Award Presented

On Dec. 17, Tom Kizzia and Rich Chiappone visited the library to talk about history and writing, drawing a crowd of 63 people. Tom Kizzia was presented with a State of Alaska legislative citation honoring his contributions to Alaskan literature. The award was presented by Representatives Andrew Gray and Sarah Vance.

Notable Work Anniversaries

In December we had two notable work anniversaries to celebrate. Chief Robl celebrated 40 years with the City and Bryan Hawkins celebrated 25 years with the City. Your commitment and excellence over the years have made a lasting impact—thank you both for all that you do!

Celebrating Kristen Faulkner

On Dec. 27, the City partnered with the Chamber of Commerce for an event celebrating Kristen Faulkner, Homer's very own Olympic medalist! On a visit home for the holidays, Kristen welcomed the community to Homer High School Mariner Theatre for a heartwarming Q&A session, with Jim Anderson, Jon and Sara Faulkner, and former Mayor Ken Castner. Kristen was presented with a City of Homer Award of Excellence

from former Mayor Castner. She was also presented with a State of Alaska legislative citation from Representative Sarah Vance.

Karen Hornaday Park Campground

With the recent mild winter weather Parks Maintenance Coordinator Chad Felice has been able to do some cleaning up at the Karen Hornaday Park Campground. The campground has been closed for a few years and the alders have taken over the campsites and roadway. Prior to the closure the City was having problems with illegal camping and other activities in the campground because the amount of alder and brush made it easy to hide out. The City has also heard feedback that the overgrowth made the park area feel unsafe for the kids playing on the playground. With the help of Public Works equipment operators, work is being done to selectively clear out the alder overgrowth and open up lines of sight around the campground. I walked the area with Chad, Public Works Superintendent Mike Zelinski, and Public Works Director Dan Kort this past Wednesday. Most campsites now have great views so campers can see the bay, watch a ballgame, or see their kids on the playground, and there will still be some buffer between campsites when the trees and remaining alders leaf out in the spring and summer. When the selective alder clearing is complete there will be areas where Parks can make improvements with landscaping and selective tree plantings. Stump removal around the campground is planned, along with some additional clearing and ditching below to help with drainage. We will be discussing options for opening the Karen Hornaday Campground during our departmental budget discussions, with a timeframe still to be determined.

There have been questions about some clearing that has been done near the park area on the hospital side of Woodard Creek. The City is not working in that area; it is right of way clearing along the power lines by Carlos Tree Service for Homer Electric Association.

Landslide Hazard Susceptibility Reporting

The Alaska Division of Geological & Geophysical Surveys (DGGS) has finished mapping landslide hazard susceptibility for the City of Homer and nearby Kachemak City. These maps are designed to help local officials and the public better understand areas that could be at risk for slope failures. They're also meant to support long-term regional planning, boost resilience, and guide updates to Homer's Comprehensive Plan.

While the maps don’t predict future landslides, they highlight spots where landslides have happened in the past and recommend areas where further geotechnical studies might be needed, especially if development is planned.

Attachments:
State of Alaska Press Release DGGS publishes Homer landslide hazard susceptibility maps
Landslide Hazard Susceptibility Mapping in Homer, Alaska Executive Summary
Landslide Hazard Susceptibility Mapping in Homer Report
Landslide Maps

John Boyle
Commissioner

Department of
Natural Resources

dnr.alaska.gov

Anchorage, Alaska

STATE OF ALASKA

PRESS RELEASE

For Immediate Release: December 11, 2024

DGGS publishes Homer landslide hazard susceptibility maps

(Fairbanks, AK) – The Alaska Division of Geological & Geophysical Surveys (DGGS) has completed landslide hazard susceptibility mapping for the City of Homer and neighboring Kachemak City. The report is available here: https://doi.org/10.14509/31155.

The results are intended to educate officials and the public regarding locations of potential slope failure hazards, provide a basis for regional long-term planning and resilience, and to inform the City of Homers' update of their Comprehensive Plan.

"We're pleased that our partnership with DGGS brought these much-needed FEMA funds to Homer," said Julie Engebretsen, acting City Manager. "Our Planning Commission and City Council will use the new lidar data and landslide susceptibility report as resources while we work on slope stability issues in the coming years."

DGGS received funding in 2018 from the Federal Emergency Management Agency (FEMA) Cooperating Technical Partners program to conduct the work, which included collection of new high-resolution light detection and ranging (lidar) elevation data.

"DGGS is excited to make this new study available to the Homer community, which represents the first landslide susceptibility maps and report published by the agency," said Melanie Werdon, DGGS Director and State Geologist. "This project predates the Alaska Landslide Hazards Program, established in 2023 to provide actionable science to communities that are affected by landslides."

These maps do not predict slope failures but depict locations where landslides have occurred and where additional geotechnical investigations are suggested if the area is targeted for development. DGGS is dedicated to mapping and assessing landslides, understanding and quantifying landslide hazards, and improving geologic hazard communication and coordination with other agencies and communities.

This report complements a 2022 coastal bluff stability assessment for Homer, also published through DGGS: https://doi.org/10.14509/30908.

The Department of Natural Resources' mission is to develop, conserve, and maximize the use of Alaska's natural resources consistent with the public interest.

Media Contact: Lorraine Henry 907-378-4926 lorraine.henry@alaska.gov

###

Stay connected:

DGGS on Facebook and X: @akdggs

DNR Newsroom: http://dnr.alaska.gov/commis/dnr_newsroom.htm

DNR on Social Media: http://dnr.alaska.gov/commis/social_media.htm

DNR Public Information Center: http://dnr.alaska.gov/commis/pic/

Landslide Hazards Susceptibility Mapping in Homer, Alaska—Executive Summary

- In the 2017 Risk Report for the Kenai Peninsula Borough, the City of Homer identified slope failures as a concern with a Recommended Resilience Strategy of completing a comprehensive slope failure hazard assessment for the city.
- To support the City of Homer's resilience to potential hazards, the Alaska Division of Geological & Geophysical Surveys (DGGS) received funding from the Federal Emergency Management Agency (FEMA) Cooperating Technical Partners (CTP) program to create a map and database of existing slope failures, maps of shallow and deep-seated landslide susceptibility, and a map of simulated debris flow runouts for the City of Homer and neighboring Kachemak City. (https://doi.org/10.14509/31155)
- The landslide inventory integrates existing maps of prehistorical landslides, those caused by the 1964 Great Alaska Earthquake, and newly mapped slope failures identified in sequences of aerial photographs since 1950 and high-resolution light detection and ranging (lidar) data collected for the project. (https://doi.org/10.14509/30591)
- DGGS created shallow and deep landslide susceptibility maps following protocols like those developed by the Oregon Department of Geology and Mineral Industries, which includes incorporating landslide inventory data, basic geotechnical soil properties, and lidar-derived slope steepness.
- Debris flow runout extents were generated using the model Laharz, which simulates runouts based on catchment-specific physical parameters (for example, hypothetical sediment volumes).
- Data from these analyses are collectively intended to depict locations where landslides are relatively more likely to occur and to model the extent of their potential impacts. The maps are not intended to predict slope failures, and site-specific, detailed geotechnical investigations should be conducted prior to development in vulnerable areas.
- The intended use of these overview maps is to help identify slopes with a relatively high slope failure hazard in and around Homer, to provide a basis for regional, long-term planning and increased resilience, and to help identify localities where more detailed mapping is warranted if areas are to be developed or improved. Maps are not intended to be used for legal, engineering, or surveying purposes.
- DGGS developed the landslide inventory, shallow landslide susceptibility, deep landslide susceptibility, and debris flow runout maps using the best available data at the time of the project; however, there are many inherent limitations. Conditions that lead to a landslide are complex. Some influencing factors like geologic and hydrologic conditions, vegetation, seasonal weather, and long-term climate all change at different rates while other landslide triggers, like earthquakes, are unpredictable. As such, there is potential for areas not depicted on these maps to be affected by future landslides.
- This report complements a 2022 Coastal Bluff Stability Assessment for Homer, also published at DGGS (https://doi.org/10.14509/30908).

For more information contact:
Dr. Barrett Salisbury, DGGS, barrett.salisbury@alaska.gov
dggs.alaska.gov

Report citation:
Salisbury, J.B., 2024, Landslide hazard susceptibility mapping in Homer, Alaska: Alaska Division of Geological & Geophysical Surveys Report of Investigation 2024-3, 21 p., 3 sheets. https://doi.org/10.14509/31155

Report of Investigation 2024-3

LANDSLIDE HAZARD SUSCEPTIBILITY MAPPING IN HOMER, ALASKA

J. Barrett Salisbury

Aerial photograph looking south towards the Homer Spit.

Published by
STATE OF ALASKA
DEPARTMENT OF NATURAL RESOURCES
DIVISION OF GEOLOGICAL & GEOPHYSICAL SURVEYS

LANDSLIDE HAZARD SUSCEPTIBILITY MAPPING IN HOMER, ALASKA

J. Barrett Salisbury

Report of Investigation 2024-3

State of Alaska
Department of Natural Resources
Division of Geological & Geophysical Surveys

STATE OF ALASKA
Mike Dunleavy, Governor

DEPARTMENT OF NATURAL RESOURCES
John Boyle, Commissioner

DIVISION OF GEOLOGICAL & GEOPHYSICAL SURVEYS
Melanie Werdon, State Geologist and Director

Publications produced by the Division of Geological & Geophysical Surveys (DGGS) are available for free download from the DGGS website (dggs.alaska.gov). Publications on hard-copy or digital media can be examined or purchased in the Fairbanks office:

Alaska Division of Geological & Geophysical Surveys
3354 College Rd., Fairbanks, Alaska 99709-3707
Phone: (907) 451-5010 Fax (907) 451-5050
dggspubs@alaska.gov | dggs.alaska.gov

DGGS publications are also available at:
Alaska State Library,
Historical Collections & Talking Book Center
395 Whittier Street
Juneau, Alaska 99811

Alaska Resource Library and Information Services (ARLIS)
3150 C Street, Suite 100
Anchorage, Alaska 99503

Suggested citation:
Salisbury, J.B., 2024, Landslide hazard susceptibility mapping in Homer, Alaska: Alaska Division of Geological & Geophysical Surveys Report of Investigation, 21 p., 3 sheets. https://doi.org/10.14509/31155

Contents

Figures

Tables

Map Sheets

LANDSLIDE HAZARD SUSCEPTIBILITY MAPPING IN HOMER, ALASKA

J. Barrett Salisbury

Abstract

The potential for slope failures poses a great safety and financial risk to people and infrastructure in many communities throughout Alaska, including the City of Homer. The Alaska Division of Geological & Geophysical Surveys (DGGS) completed a comprehensive landslide hazard assessment for the city by creating a map and database of historical and prehistoric slope failures, maps of shallow and deep-seated landslide susceptibility, and a map of simulated debris flow runouts for the City of Homer and neighboring Kachemak. The landslide inventory map integrates existing maps of landslides caused by the 1964 Great Alaska Earthquake and newly mapped slope failures identified in sequences of aerial photos since 1950 and high-resolution light detection and ranging (lidar) data collected for this project. DGGS created a shallow landslide susceptibility map following protocols like those developed by the Oregon Department of Geology and Mineral Industries, which includes incorporating landslide inventory data, geotechnical soil properties, and lidar-derived topographic slope to calculate the Factor of Safety (FOS)—a proxy for landslide susceptibility. Debris flow runout extents were generated using the model Laharz, which simulates runout extents based on catchment-specific physical parameters (e.g., hypothetical sediment volumes). Data from these analyses are collectively intended to depict locations where landslides are relatively more likely to occur or are relatively more likely to travel. The results provide important hazard information that can help guide planning and future risk investigations. The maps are not intended to predict slope failures, and site-specific, detailed investigations should be conducted prior to development in vulnerable areas. Results are for informational purposes and are not intended for legal, engineering, or surveying uses.

INTRODUCTION

In the 2017 Risk Report for the Kenai Peninsula Borough, the City of Homer identified slope failures as a concern with a Recommended Resilience Strategy of completing a comprehensive slope failure hazard assessment for the city (Alaska Department of Commerce, Community, and Economic Development, 2017). To support the City of Homer's resilience to potential hazards, the Alaska Division of Geological & Geophysical Surveys (DGGS) received funding in 2018 from the Federal Emergency Management Agency (FEMA) Cooperating Technical Partners (CTP) Program to create a map and database of existing slope failures, maps of shallow and deep-seated landslide susceptibility, and a map of simulated debris flow runouts for the City of Homer and neighboring Kachemak City (fig. 1). The results of this study are intended to: 1) educate officials regarding locations of potential slope failure hazards; 2) provide information to inform future zoning and planning decisions; and 3) to inform the city's update of their Comprehensive Plan. For the area of interest (AOI) that includes the City of Homer, Kachemak City, and parts of Diamond Ridge, DGGS produced new, high-resolution (0.5 m per pixel) light detection and ranging (lidar)

[1]Alaska Division of Geological & Geophysical Surveys, 3354 College Rd., Fairbanks, Alaska 99709-3707.

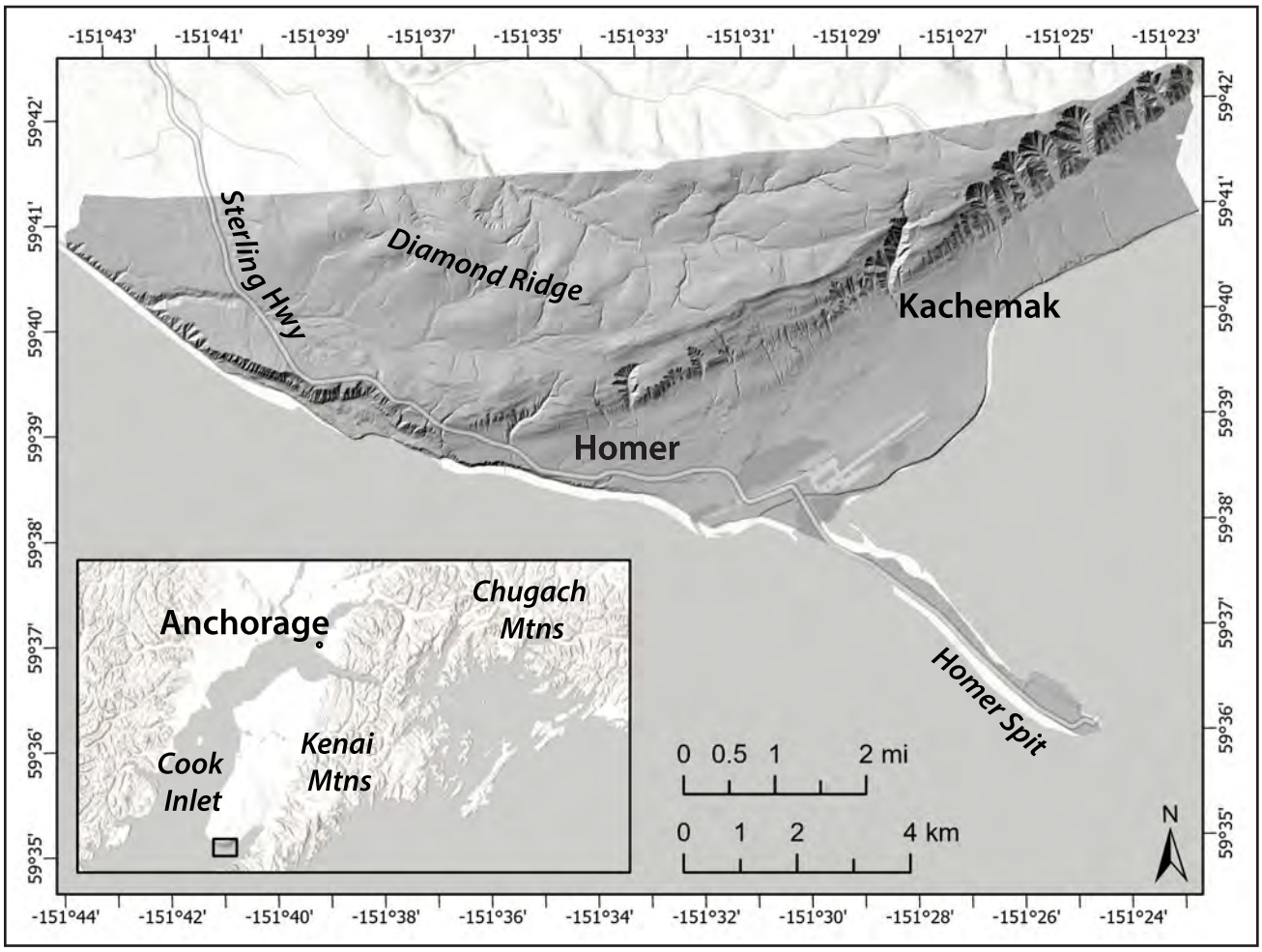

Figure 1. 2019 lidar extent (visible as a gray hillshade) and area of interest for Homer slope failure susceptibility assessment. Inset map shows study location on the western Kenai Peninsula.

elevation data and data layers specific to the AOI's slope failure hazards (Salisbury and others, 2021). This report describes the datasets and methods used for the resilience study and discusses mapping and modeling results that will be used to increase Homer's resilience to future slope failures.

BACKGROUND

Geologic Setting

Regionally, the Homer area falls within an accretionary wedge of sediments and sedimentary rocks lying above the Alaska-Aleutian subduction zone, where the Pacific plate is being subducted beneath the North American plate. The bedrock at the southern end of the Kenai Peninsula consists of moderately indurated, freshwater Eocene sands, silts, clays, and minor amounts of conglomerate in generally thin and intergraded beds and lenses (Barnes and Cobb, 1959). Known collectively as the Kenai Group, these beds contain many subbituminous coal and lignite deposits from a few inches to 7 ft (2.1 m) thick that decrease in abundance and thickness to the north. Strata are generally flat or gently dipping northward less than about 10 degrees, and the coal and lignite beds act as aquitards, impeding the vertical movement of groundwater. The total thickness of the Kenai Group likely exceeds 4,700 ft (1,430 m) (Barnes and Cobb, 1959; Wilson and Hults, 2012). In general, the soils of Homer are mapped as silt loam with slight compositional variations owing to the nearly ubiquitous parent material. Exceptions include organic-rich wetland soils, beach deposits, or steep cliffs where erosion prevents soil formation (United

States Department of Agriculture [USDA] Natural Resources Conservation Service [NRCS], 2005).

The structure of the Kenai Group in Homer consists of northeast-trending broad folds. These folds (with limb dips less than ~10 degrees) are superposed on the northeast-trending regional forearc basin that defines Cook Inlet. Many high-angle faults have been mapped in wave-cut beach bluffs, but little is known about the extent of these northwest-striking features. In general, faults show a normal sense of displacement, are steep to sub-vertical, and have vertical displacements ranging from a few inches to nearly 80 ft (24.4 m) (Barnes and Cobb, 1959). While none of these fault offsets found in Tertiary rocks are the result of Holocene surface deformation, we cannot rule out the possibility that shallow, crustal faults exist in the active accretionary wedge at the modern plate boundary.

The physiography of Homer is characterized by a prominent, steep escarpment of moderately cemented Tertiary sedimentary bedrock. The escarpment is a result of glacial scour by the Kachemak Bay ice lobe during the recent Moosehorn and Killey stades of the Naptowne glaciation, approximately 23 and 18 thousand years before present, respectively. The escarpment is dissected by steep canyons, and the gently sloping lowlands below are underlain by a mix of canyon-fed debris flow deposits and drift (i.e., Pleistocene sediments transported/deposited by glacial ice or meltwater) from the last major glaciation (Reger and others, 2007).

Types of Slope Failures

The term "landslide" is a commonly used catch-all term for gravity-driven mass movements. However, "landslide" refers to a range of movements, including slides, flows, falls, topples, and spreads (Cruden and Varnes, 1996) (fig. 2). A "slide" typically moves downslope along one or more failure planes, sometimes without much internal deformation. "Flows" move rapidly downslope as a viscous

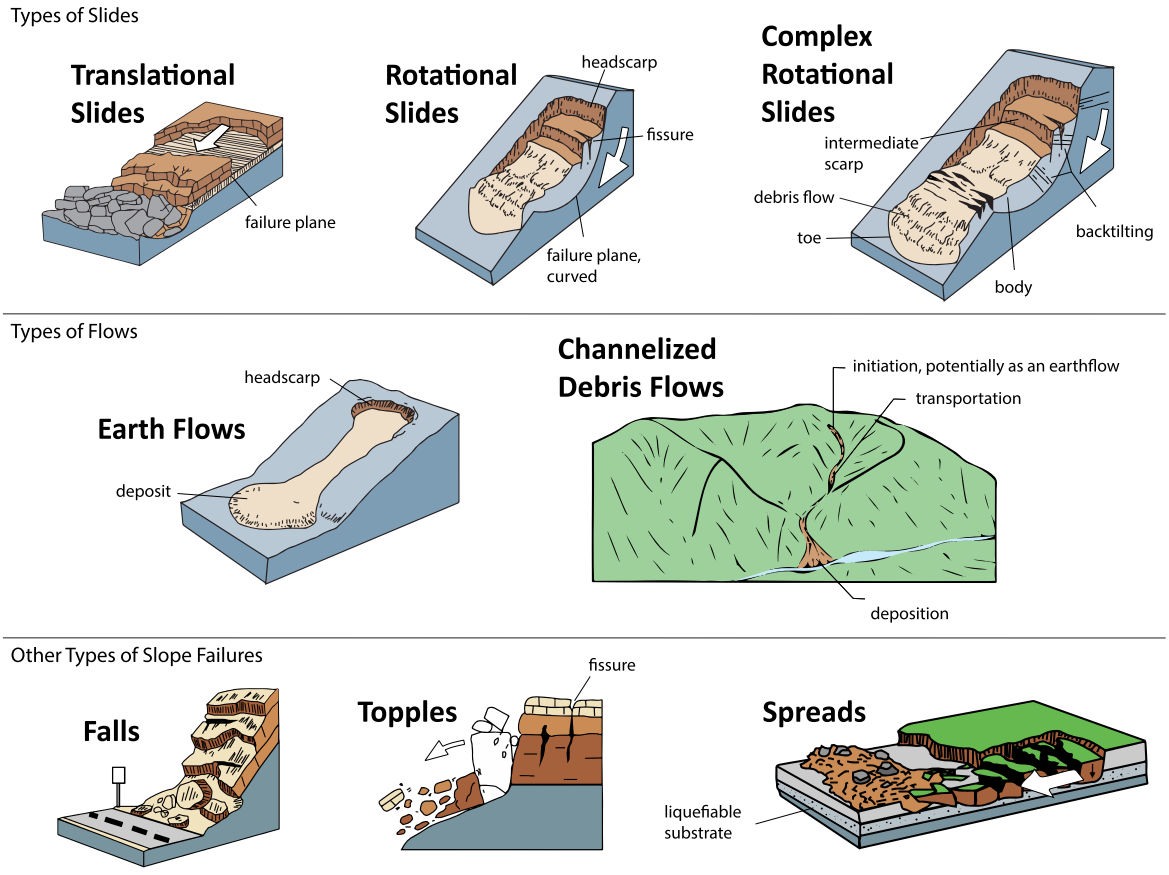

Figure 2. Types of slope failures as classified by Varnes (1978). Illustrations modified from Cruden and Varnes (1996) and Highland and Johnson (2004).

fluid because of water content and/or loss of cohesion within a moving mass. In and around Homer, there is evidence of several types of slides, flows, and complex mixes of the two.

Slides

Slides can occur in a wide range of geologic materials and typically occur on slopes of 20 to 40 degrees. Downslope movement occurs on one or more distinct failure planes, and a slide mass may travel with very little internal deformation. A translational landslide moves down (and potentially outward) along a planar failure surface without backwards tilting (fig. 2). Translational slides are typically shallower and move longer distances than rotational slides. A rotational slide moves along an upward-curved (i.e., spoon-shaped) failure plane such that the slide mass tilts backwards towards the headscarp (fig. 2). Both types of landslides, while initially sliding as a more-or-less coherent block, may disintegrate to rubble or transition to a flow, depending on local conditions. In either case, triggering mechanisms include saturation of slopes and increased water levels within the mass due to intense or prolonged rainfall or snowmelt, and human-induced or natural slope disturbances such as undercutting (e.g., removing the toe of an existing slope) or earthquake shaking (Cruden and Varnes, 1996; Highland and Bobrowsky, 2008).

Flows

Earthflows generally occur in fine-grained soils, including silts and clays, and exhibit a wide range of relative sizes, failure depths, and velocities. Earthflows typically have a characteristic hourglass shape, leaving behind a bowl or depression at the head of the slope failure, often with a headscarp (fig. 2). In Homer, flows typically occur on steep slopes within drainage catchments and range from hundreds to tens of thousands of square feet in area (tens to thousands of square meters). Ground observations and historical aerial photographs show that these earthflows likely initiate as small-scale slides that tend to be relatively shallow, mostly affecting the uppermost hydrologically active part of the soil column (approximately 5 ft [1.25 m]). Earthflows typically move as plastic or viscous masses with strong internal deformation, because they are commonly triggered by saturation of soil due to prolonged or intense rainfall or snowmelt, earthquakes, or human-induced vibration (Keefer and Johnson, 1983). In Homer, daylighting coal beds in coastal bluffs and steep catchments act as aquicludes, and natural springs from above them, which may locally contribute to earthflow initiation.

Channelized debris flows occur on steep, concave slopes and are initiated as earthflows (or other types of landslides) that run into a channel and gain momentum by picking up more debris, water, or speed (fig. 2). Channelized debris flows are prevalent in steep gullies, particularly in areas of weak soil. These types of movements are typically initiated by heavy surface-water flow or in areas where earthflow conditions are common; they can move downslope rapidly, approaching 35 miles per hour (56 km per hour) (Cruden and Varnes, 1996; Highland and Bobrowsky, 2008). Even though channelized debris flows may be thin and watery, they can incorporate large boulders, vegetation, and other objects. Coupled with their sudden onset, even small debris flows can be lethal.

The debris flows that emanate from the bedrock-walled canyons and gullies deposit material on alluvial fans within and below the mouths of the canyons. The alluvial fan deposits have a fine-grained, silt and sand matrix and contain blocks of coal, cobbles, and plant debris of all sizes (Reger and others, 2007). Each fan is composed of many individual debris flow deposits, and some flows deposit materials beyond the fan limits in existing ephemeral stream channels. The debris flows are supply-limited phenomena, meaning each event effectively empties the source area (or drainage gulley) of accumulated debris (Reger and others, 2007). The debris flow requires (1) sufficient time since the previous flow to accumulate sufficient debris in the source canyon and (2) a hydroclimatic event of sufficient duration or magnitude to saturate and mobilize the debris accumulated in the canyon (Jakob, 2005). Events are often initiated by a small earthflow from a steep

canyon wall, and this slide imparts an initiating pulse of material and energy to the existing unstable sediment in the canyon channels. Recurrence intervals are estimated to range from decades to centuries, with smaller events typically occurring more frequently than large events (Reger and others, 2007).

Bluff Point Landslide

The Sterling Highway at the western edge of Homer city limits closely follows the headscarp outline of the Bluff Point landslide (red line, fig. 3). The Bluff Point landslide is the largest landslide of the Kenai Peninsula lowland and is approximately 3.4 mi (5.4 km) long, up to 1.6 mi (2.6 km) wide, and has a scarp, or cliff relief, of 200 to 600 ft (60–215 m) (Reger and others, 2007). The Baycrest/Homer Overlook Point offers a view to the southwest, down across the ponded area of the back-tilted landslide block (fig. 3, yellow area) that formed as the mass slid along one or more spoon-shaped failure planes at depth. Bathymetry of the seafloor in this area suggests that the main body of the landslide could have extended up to 1.2 mi (2 km) out from the modern shore (Reger, 1978), as also evidenced by exposures of basal shear surfaces in the beach far out from the modern bluff. Sediment layers at the modern shoreline are noticeably back-tilted, as opposed to the relatively flat-lying layers of the main bluff (figs. 2 and 3).

The landslide could have occurred any time since about 17,500 years before present (BP), when

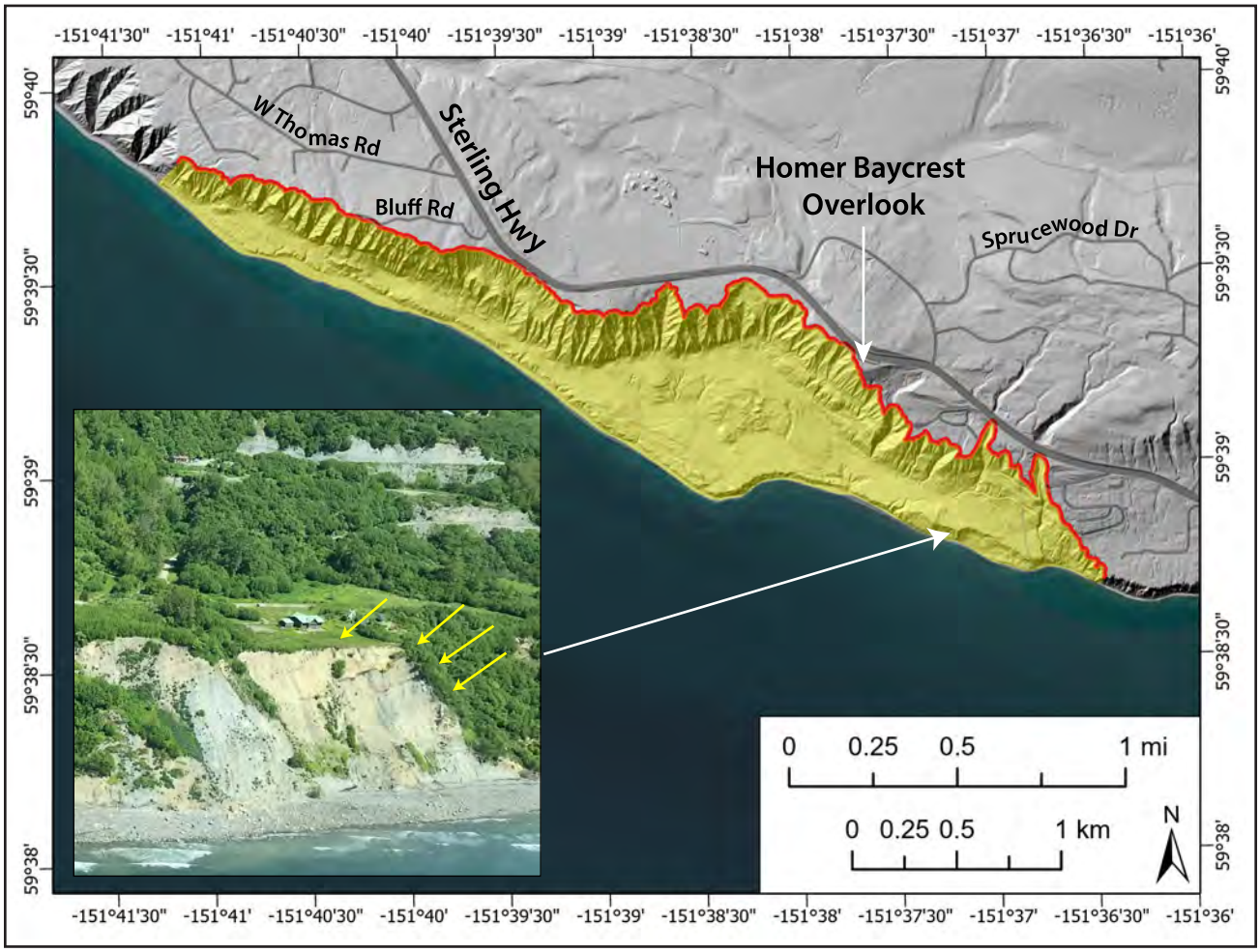

Figure 3. Bluff Point landslide headscarp extent (red line) along the Sterling Highway in the 2019 lidar-derived hillshade (Salisbury and others, 2021). Note that the headscarp has undergone significant erosion since formation ~2,250 years ago. The yellow area represents the headscarp wall and back-tilted landslide block. Inset: oblique aerial photograph of back-tilted coal seams within the landslide mass.

the Killey-age glaciers retreated from the Bluff Point area back into Kachemak Bay, effectively debuttressing (i.e., destabilizing) the slope. Radiocarbon age estimates of vegetation from a soil layer overrun by the landslide suggest the slide occurred about 2,250 BP (Berg and others, 2014). Though there is no direct evidence linking the Bluff Point landslide to a causative subduction zone earthquake, it is plausible that this massive bluff failure was triggered by such an event. Shennan and Hamilton (2006) analyzed fossil diatoms within peat-mud couplets to reconstruct land/sea-level changes for the 1964 and five earlier great earthquakes during the past 3,300 years, two of which occurred about 2,100 BP and 2,500 BP. Given the uncertainties associated with radiocarbon dating, it is possible (though not proven) that either of these earthquakes triggered the bluff collapse.

The slide block has been extensively modified by coastal processes since deposition, and therefore, it is not clear whether the Bluff Point landslide occurred as a single, catastrophic failure or as a series of progressive, smaller failures. The remnants of the original landslide block are continuously eroding and collapsing, and there is evidence that reactivation of old slump blocks is possible, with at least one portion of the old slump block having been active as recently as 2009 (Berg, 2009). Deep-seated landslides fail progressively over time, and—coupled with the potential for strong shaking in 1964-type subduction zone earthquakes—future failures of the headwall are inevitable (Reger and others, 2007).

Effects of the Great Alaska Earthquake, 1964

The effects of the March 27, 1964, Great Alaska Earthquake in the Homer area were thoroughly documented after the event. Observations included general damage caused by tectonic subsidence and earthflows, landslides, fissures, seiches, submarine landslides, and beach changes caused by strong ground shaking during the M9.2 event (Waller, 1966). While the earthquake effects in Homer were minor compared to devastation in other parts of Alaska, most of the seismic damage to the community occurred on Homer Spit because of tectonic subsidence (2–3 ft [0.6–0.9 m]) and differential compaction and lateral spreading (an additional 1–4 ft [0.3–1.2 m]) (Plafker, 1969). Similarly, there were several areas of heightened coastal erosion in the months and years following the earthquake. This report focuses on the Bluff Point landslide headscarp and other inland areas where there were several instances of earthquake-induced geologic effects throughout the community.

Despite "the incompetent nature of the bedrock and of the thin layer of soil that overlies the rock," Waller (1966) notes that, surprisingly, only one landslide and one earthflow of significance occurred in Homer during the 1964 earthquake, both north of Kachemak City. The landslide occurred as the collapse of a precipice between two steep, neighboring catchments eroding into the Kenai Group (fig. 4C, labeled 1964 event on the right). The landslide block disintegrated and spread into a debris apron approximately 600 feet (183 m) long and 100 feet (30 m) wide below the existing precipice. Waller (1966) stresses that "landslide hazards exist in comparable situations near Homer—and indeed anywhere that promontories extend out from precipitous bluffs and cliffs."

The earthflow and channelized debris flow runout occurred in the neighboring drainage catchment southwest of the landslide (fig. 4C, labeled 1964 event on the left).

> It created a jumbled mass of uprooted trees, mudflows, rafts of soil and vegetation, and collapsed ground. The area of disturbed ground [was] about 1,000 feet [305 m] long and [had] a maximum width of about 400 feet [122 m]. Horizontal displacement of material within the flow, however, probably did not exceed 200 ft [61 m]. The material involved [consisted] mainly of silt, some fine sand, and occasional layers of flat pebbles. The head of the flow is near the apex of

> an alluvial fan at the mouth of a small canyon occupied by an intermittent stream. Water was seeping from both disturbed and undisturbed material… and may have contributed to causing the flow. (Waller, 1966).

Lastly, the earthquake caused many fissures throughout Homer, the most notable of which occurred near the headscarp of the Bluff Point landslide at a U.S. Bureau of Land Management field station built 50 ft (15 m) from the edge of the 700 ft (213 m) bluff. In general, a fissure is an opening crack that forms at the ground surface. Regarding earthquakes, fissures may be caused by several different mechanisms, including primary on-fault deformation or secondary off-fault deformation. The fissures that formed in Homer in 1964 are secondary effects of the earthquake (i.e., caused by seismic shaking) and represent the geomorphic expression of lateral spreads (perhaps due to liquefaction), subsidence from sediment compaction, the initiation of new landslides, or triggered movements on existing, retrogressive landslides (e.g., fig. 2, rotational slides, topples).

> Numerous fissures developed during the earthquake on the surface above the bluff, some of them several inches wide. A few could be traced about 20 ft [6 m] down the bluff face. One earth fissure extended across the area of a field-station building and cracked the basement floor of the structure. Areas above and below promontories where earthslides might occur must remain suspect as sites for any building. (Waller, 1966).

Other anecdotal reports suggest that fissures at the mouth of Thurston Canyon were so large that "a Shetland pony fell into one several days after the earthquake and could not get out," but these observations were not checked in the field (Waller, 1966).

Homer is located above a boundary between segments of the earthquake-generating Alaska-Aleutian subduction zone—the Kodiak Island (KI) segment to the southwest and the Prince William Sound (PWS) segment to the northeast. While the 1964 Great Alaska Earthquake ruptured both the KI and PWS segments, recent paleoseismological findings from around the region suggest that the two segments may rupture independently. Research by Shennan and others (2014) suggests that the average recurrence interval for great (M>8) megathrust earthquakes on the PWS segment is approximately 535 years, a slightly shorter recurrence interval than the 589 years estimated by Carver and Plafker (2008). Importantly, however, work in the KI segment revealed evidence for more frequent megathrust earthquakes than the PWS segment (Nishenko and Jacob, 1990), and recurrence intervals for M7.5–8.0 earthquakes may be as low as 60 years in this area (Nishenko, 1991). The fact that there has been a significant historical earthquake in the area does not reduce the likelihood that there may be another earthquake at any time.

For context, peak ground accelerations (PGAs, the maximum ground shaking that occurs during an earthquake) in Homer during the M9.2 Great Alaska Earthquake reached about 0.35g, or 35 percent of the acceleration due to Earth's gravity (U.S. Geological Survey [USGS] ShakeMap). However, time-independent Probabilistic Seismic Hazard Models—models that quantify the rate at which ground-motion levels at a site are exceeded—show a 2 percent chance in 50 years (the rough equivalent of an earthquake with a ~2,500-year return period) for PGAs of approximately 0.6g in Homer (Wesson and others, 2007). The potential for future strong ground motion should not be underestimated.

METHODS

The Oregon Department of Geology and Mineral Industries published a series of special papers detailing protocols for inventory mapping of landslide deposits from lidar, shallow landslide susceptibility, and deep landslide susceptibility (Burns and Madin, 2009; Burns and others, 2012; Burns and Mickelson, 2016, respectively). Where

existing geologic and geotechnical soils data allow, we closely follow these suggested methods and build on other similar landslide hazard studies conducted by DGGS (e.g., Hubbard and others, 2024).

Lidar Acquisition and Processing

DGGS used lidar point cloud data to produce a high-resolution (1.6 ft [0.5 m]) digital terrain model (DTM) and a digital surface model (DSM) for Homer (Salisbury and others, 2021). The DTM, also known as a bare-earth elevation model, was essential for identifying landslide geomorphology beneath dense vegetation, confirming evidence of landslide activity identified in aerial photograph sequences, making Factor of Safety (FOS) calculations, and modeling potential debris flow runouts. DGGS operates a RIEGL VUX1-LR scanner integrated with a Global Navigation Satellite System (GNSS) and Northrop Grumman Inertial Measurement Unit. The lidar and the GNSS data were collected on June 3, 2019, and processed using TerraSolid software. The Alaska Division of Mining, Land and Water's Survey Section conducted a targeted Ground Control Survey for this project June 19–20, 2019. The resulting modeled surfaces reveal the complex topography required for slope failure interpretation and modeling. These data are available as a Raw Data File with an open end-user license. All files are available via the DGGS elevation portal at elevation.alaska.gov. See Salisbury and others (2021; doi.org/10.14509/30591) for additional metadata.

Landslide Inventory

There are few publications with comprehensive landslide catalogs near Homer, despite numerous examples of historical debris flows emanating from the steep bluffs and blocking roads in Homer. These events, typically caused by heavy rains or rain-on-snow events, cause flooding, blockage, and damage to roads, and damage to culverts and other water diversion structures.

The comprehensive landslide inventory presented here (sheet 1) spans 1952–2019 and was generated by (1) collecting and organizing existing information about previously identified landslides; (2) obtaining, georeferencing, and analyzing sets of aerial photographs since 1952; (3) acquiring, processing, and analyzing high-resolution lidar elevation data; (4) compiling all landslide information into a geodatabase; and (5) generating a landslide inventory map.

The most prominent landslide in the area, the Bluff Point landslide, has been well-known for some time. The Bluff Point headland was originally named by W.H. Dall of the U.S. Coast and Geodetic Survey in 1880. Early exploration in the southwestern Kenai Lowland was motivated by potential coal resources, and while the Bluff Point headland was mentioned in several reports in the following decades, the first instance of it being mapped as a paleo-landslide was in a USGS description of the Tertiary stratigraphy and associated coal resources in the area by Barnes and Cobb (1959). It has since been recognized in guidebooks and several news articles, and more recent work has helped refine the age estimate for the slide. The only other documentation of slope failures in the area followed the 1964 Great Alaska Earthquake (e.g., Waller, 1966), as mentioned above.

DGGS acquired multiple epochs of historical aerial photographs from the USGS Earth Explorer (earthexplorer.usgs.gov) and the Kenai Peninsula Borough Historical Imagery Viewer (gis.kpb.us/map/index.html?viewer=imagery). We chose years, or combinations of closely spaced years, with complete aerial coverage of upland Homer and Kachemak City while maximizing the number of distinct intervals since 1952. The photograph sets used are from 1952, 1975, 1984/1986, 2000, 2012–2013, and 2016 and were georeferenced in ArcGIS Pro.

For the Bluff Point landslide and all upland catchments, slope failure scars were delineated by comparing sets of aerial photographs. Interpreting slope failure scars from aerial photographs relied on the assumption that there is a one-to-one correlation between a newly identified scar and an earthflow

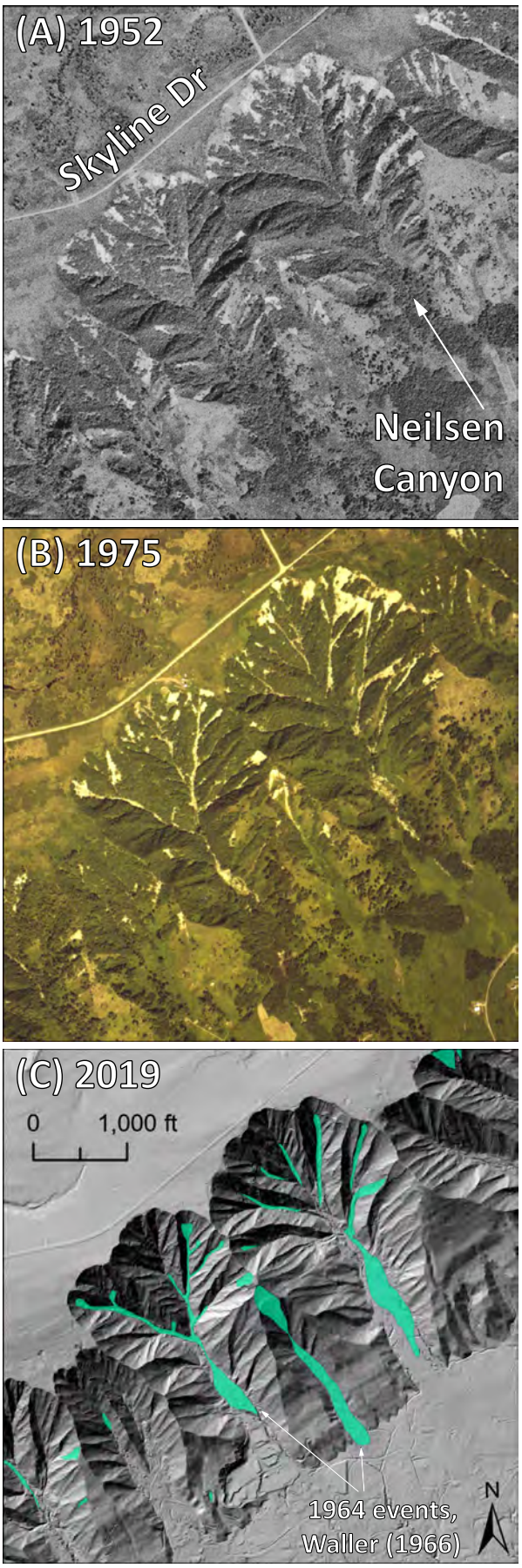

or debris flow event (fig. 4). We initially calibrated earthflow and debris flow identification using aerial photographs by analyzing the topographic expression of the slides that are known to have occurred during the 1964 Great Alaska Earthquake (fig. 4). This mapping strategy could underestimate the total number of individual slides, because the length of time required for vegetation to re-establish itself (a few years) is far exceeded by the average photo interval (~13 years). However, areas that remain unvegetated because they are oversteepened by failure or are channelized may have hosted several slides between one aerial photo epoch to the next.

Slope failure scars were delineated by digitizing the landslide footprints. To minimize positional error from distortion around the edges of the aerial photographs, landslide polygons were digitized directly on the 0.5 m, lidar-derived bare earth elevation models according to the geomorphic expression of the identified slope failures (e.g., fig. 4). At the same time, any landslide geomorphology indicative of recent instability but not visible in the air photographs was mapped as a landslide headscarp line only, as the full extent of the slide (i.e., deforestation) is difficult to determine from 2019 topography alone (fig. 5). We also mapped slope failures along the coastline, but in the 2019 lidar data only. Rarely, we also mapped debris flow deposits or runout zones with or without an immediate source area (fig. 5). These mapped features do not contain any additional date information. The slope geomorphology was mapped at about

Figure 4. A, B. Examples of georeferenced aerial photographs for two steep upland catchments where landslides were mapped by Waller (1966) after the 1964 Great Alaska Earthquake. We used changes in vegetation between air photo pairs to identify landslide, earthflow, and channelized debris flow scars. **C.** Slope failures that were identified between air photo sets were digitized in the 2019 lidar elevation data using geomorphic characteristics. Note: the channelized debris flow deposit polygons include both the source areas and runout zones (deposits). Though only two of the major events shown here are known to have occurred in the 1964 earthquake, it is likely that the channelized debris flow in Neilsen Canyon also occurred at the same time.

1:2,500, and the ArcGIS Pro feature class and associated geospatial information form the Landslide Inventory Database (fig. 6).

Shallow Landslide Susceptibility

The FOS (sheet 2) is a relationship between shear forces acting to move material downslope (e.g., gravity, unit weight) and forces acting to resist downslope movement (e.g., soil cohesion) (Cornforth, 2005). In general, the greater the forces acting to move material downhill relative to forces resisting movement, the lower the FOS and the greater the likelihood a slope failure may occur.

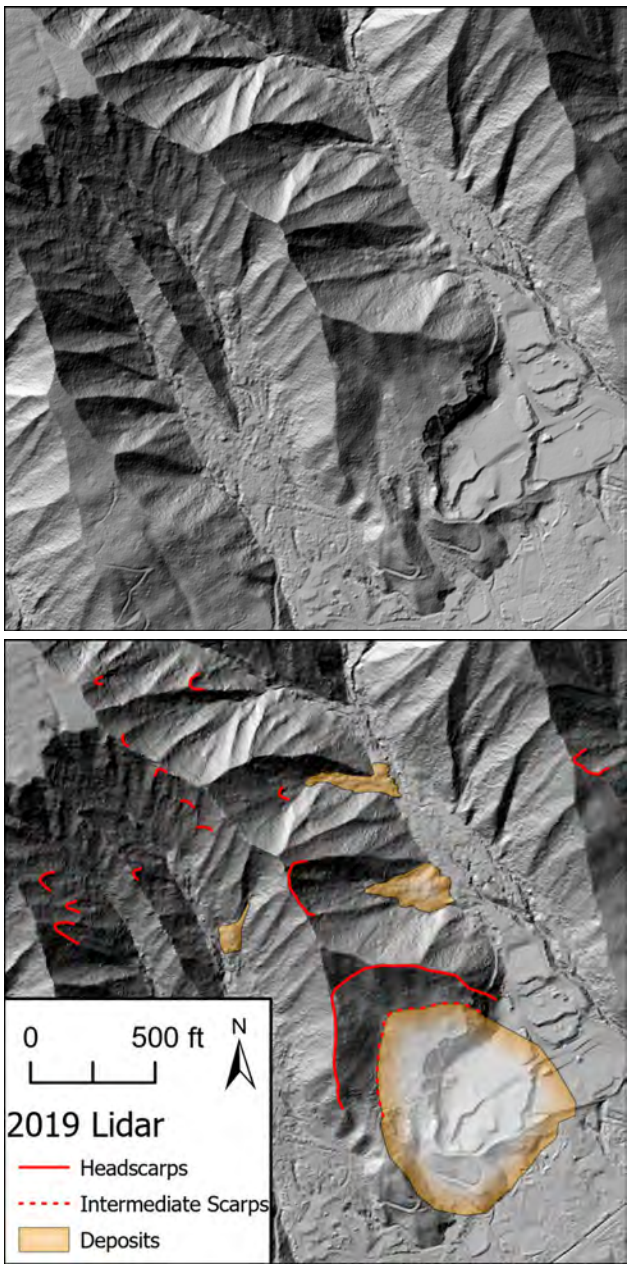

Figure 5. Excerpt of 2019 lidar landslide mapping near the end of China Poot Street. Headscarps, intermediate scarps, and deposits are only identifiable using bare-earth lidar and are not visible in aerial photographs. Some headscarps have no accompanying deposits and vice versa.

In Homer, we estimate the FOS for shallow landslides, or earthflows, that are approximately the thickness of the mapped soil column (~5 ft [1.25 m] or less, USDA NRCS, 2005). The following formula combines geotechnical information about the earth materials with the slope of the land surface from our high-resolution lidar data:

$$FOS = \frac{c'}{\gamma t \sin\alpha} + \frac{\tan\Phi'}{\tan\alpha} - \frac{m(\gamma_w)\tan\Phi'}{\gamma\tan\alpha}$$

where c' is effective soil cohesion, Φ' is the effective angle of internal friction, γ is soil density (unit weight), γ_w is groundwater density (unit weight), t is depth to failure surface, m is the groundwater depth ratio, and α is slope in degrees.

Areas with an FOS <1 are theoretically unstable because downslope stress is greater than the shear strength of the soil. FOS values equal to 1 are regarded as "critically stable"—meaning the driving and resisting forces are more-or-less balanced and the slope could fail at the slightest disturbance (e.g., a change in the water table position, vibration). Importantly, the FOS calculation involves several major assumptions regarding conditions present within a slope, so typically engineering geologists consider slopes with an FOS <1.5 to be potentially unstable. Therefore, we classify FOS values from 1.0 to <1.25 as highly susceptible to failure, values from 1.25 to 1.5 as moderately susceptible, and values >1.5 as having low susceptibility of failure (Burns and others, 2012) (fig. 7; red, orange, and no color areas, respectively).

Nearly all the mapped soil types in Homer are from the same parent material (i.e., geologic unit) and therefore have similar material properties as silt loams. However, there are slight differences in grain size distributions that ultimately affect the saturated soil density, so we use respective values to

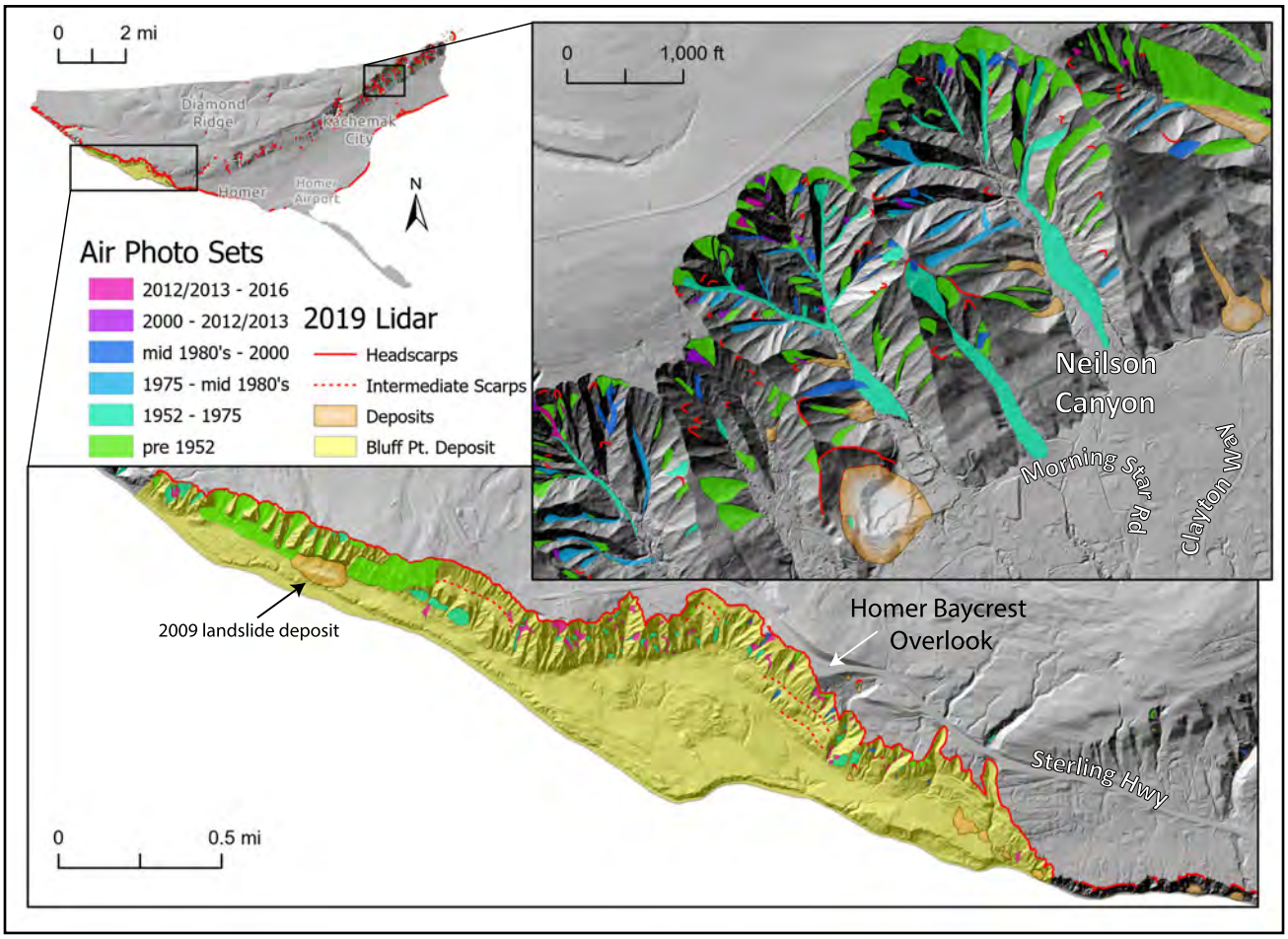

Figure 6. Excerpts from the complete landslide inventory database for the Bluff Point area (bottom) and Neilson Canyon area (top right). Earthflow and channelized debris flow scar polygons include both the source area and any associated deposit. The digital landslide inventory extends northeast of the 2019 lidar coverage into Thurston Canyon.

calculate the FOS for each group of mapped soils with the same dry unit weight (table 1). Representative angle of internal friction, cohesion, and groundwater density are assigned based on USDA-data for the western Kenai Peninsula (table 2; USDA NRCS, 2005). Geotechnical properties are assumed to be constant within individual soil units. For all calculations, we used the highest values of bulk dry density to calculate saturated bulk density, and we assumed the groundwater depth ratio to be one (implying fully saturated conditions with groundwater levels at the surface, as earthflow and debris flow events often occur following significant hydroclimatic events).

For each group of soil types (table 1), we used soil properties to calculate the FOS for a range of possible slopes (1–55 degrees), making note of slope angle thresholds corresponding to the FOS classification thresholds of 1.0, 1.25, and 1.5. We then used ArcGIS Pro Spatial Analyst toolbox to generate a slope map from the lidar-derived bare earth elevation model and extract the slope raster cells by soil type polygon. We display the data according to high (FOS 1–<1.25, red), moderate (FOS 1.25–1.5, orange), or low (FOS >1.5, no color) susceptibility to failure according to soil-specific FOS results (fig. 7). Slopes steeper than about 55 degrees are assumed to be highly unstable. We calculated the slope using a resampled, 5 m (16.4 ft) bare earth elevation model to avoid classifying small-scale, steep but low-relief features (e.g., ditches, driveway embankments) as having high susceptibility to failure.

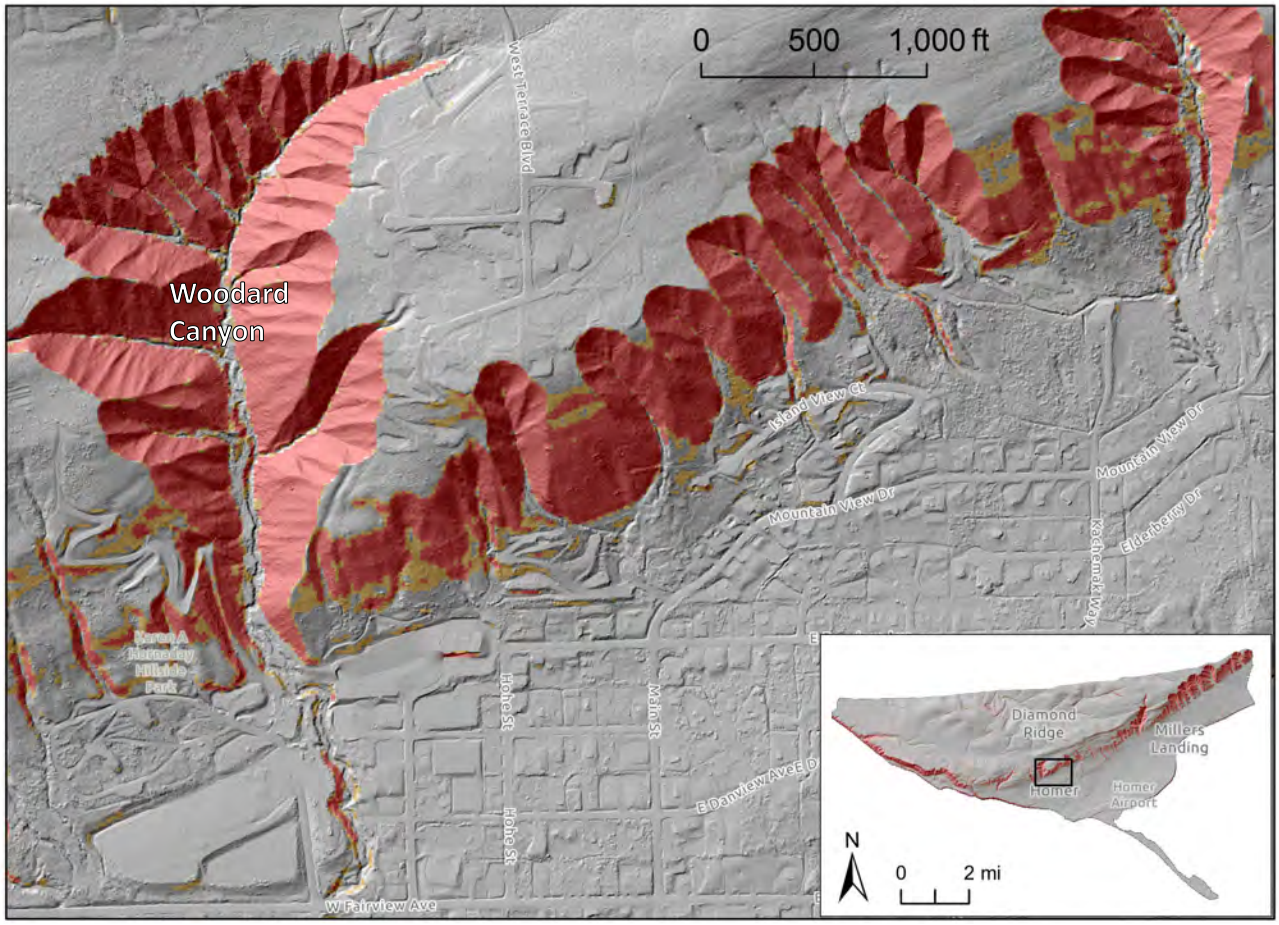

Figure 7. Excerpt from the Factor of Safety map (map sheet 2) highlighting areas of moderate (FOS 1.25–1.5, orange) and high (FOS 1–1.25, red) shallow landslide susceptibility at saturated conditions for the area near Woodard Canyon.

Deep-Seated Landslide Susceptibility

Deep-seated landslides involve the failure of materials, as the name implies, several tens of feet below layers of active soil and the uppermost weathered bedrock in an area. While the distinction between shallow and deep landslides is somewhat arbitrary, for the purposes of this report, deep slope failures include underlying lightly weathered or unweathered bedrock. In Homer, we have designated deep landslides as those that include materials below the mapped, uppermost hydrologically active soil column: for the purposes of this report, a failure surface deeper than approximately 5 ft (~1.25 m) (USDA NRCS, 2005). In general, this is a relatively shallow delineation compared to other landslide studies (Burns and Madin, 2009).

Deep landslide susceptibility is difficult to assess, but in this study area, deep-seated landslides tend to fail repeatedly and progressively. An initial, deep-seated failure weakens the strength of the local geologic material, increases permeability (resulting in an increase of water infiltration), and alters the topography by steepening toe and headscarp slopes (Burns and Mickelson, 2016). It is common for deep-seated landslides to move through retrogressive failure (i.e., continued upslope failure); therefore, the most likely locations for future deep landslides are within existing deep landslides (reactivation) or adjacent to and above existing deep landslides. Susceptibility maps rely heavily on an existing inventory of deep landslides, and all mapped deep landslide polygons and headscarp-flank polygons are considered high susceptibility areas.

Table 1. USDA Soil Series properties used in Factor of Safety calculations (USDA, 2005).

Soil Series Name	Soil Type	USDA Map Unit # in study area	Depth (in)	Dry Unit Weight (lb/ft^3)	Group
Badland Sea Cliff	silt loam	503, 504	60	1	1
null	gravel pit	563	null	2	2
null	tidal flat	688	null	2	2
null	urban	704	null	2	2
Salamatof	peat	651	60	6	3
Starichkof	peat	677, 678, 679	60	11	4
Island	silt loam	569, 570, 572	60	75	5
Mutnala	silt loam	618, 619, 620, 621, 622	60	81	6
Mutnala-Starichkof-Slikok	silt loam	623	60	81	6
Tuxedni	silt loam	700	60	81	6
Doroshin	mucky peat over silt loam	558, 559	60	87	7
Salamatof & Doroshin	peat over silt loam	650, 676	60	87	7
Truuli	muck	695	60	87	7
Beluga-Mutnala	silt loam	509	60	91	8
Kachemak	silt loam	573, 574, 575, 576, 577, 583, 584, 585	60	94	9
Smokey Bay	silt loam	657	60	94	9
Beluga-Smokey Bay	silt loam	510, 511	60	97	10
Beluga	silt loam	506, 507, 508	60	100	11
Coal Creek	silt loam	538	60	106	12
Spenard	peat over silt loam	673, 674, 675	60	106	12
Cryaquents	silt loam	701	60	106	12
Chunila	mucky silt loam	530, 531	60	112	13
Clunie	peat over silt loam	535	60	112	13
Qatal	silt loam	641	60	112	13
Slikok	peat over silt loam	653	60	112	13
Cryorthent	silt loam	703	60	112	13
Redoubt	silt loam	24	60	116	14
Cohoe	silt loam	541	60	119	15

Table 2. Generic USDA soil properties for the Soil Series in the western Kenai Peninsula (USDA, 2005).

Soil Property	Variable	Value	Unit
effective cohesion	c'	209	lb/ft^2
effective internal friction angle	Φ'	25	°
unit weight (soil)	γ	varies	lb/ft^3
unit weight (water)	γ_w	64	lb/ft^3
depth to failure surface	t	5.0	ft
proportion of slope thickness saturated	m	1.0	

In the Homer area, there are several mapped deep-seated landslides, the most prominent of which is the Bluff Point landslide. We use a headscarp buffer to highlight the area surrounding the Bluff Point landslide with high susceptibility to deep-seated landslide failure. Most poorly consolidated coarse-grained geologic materials have an angle of internal friction of at least 26 degrees. Because a slope ratio of 2 horizontal to 1 vertical (2H:1V) is equal to 26 degrees, geotechnical engineers commonly use that ratio as a proxy for slope stability (Burns and Mickelson, 2016). The maximum widespread vertical relief of the Bluff Point landslide headscarp is about

600 ft (215 m), so we add a horizontal buffer of 1,200 feet (430 m) to the scarp (fig. 8).

Procedures exist for defining areas that are moderately susceptible to deep-seated landslide failure, including identifying susceptible geologic units, geologic contacts, and engineering geologic units (Burns and Mickelson, 2016). However, given the paucity of high-resolution geologic and soils data for the area, additional analyses were beyond the scope of this study.

Debris Flow Runout Modeling

Laharz is a numerical model developed by Schilling (1998) for the USGS that simulates the behavior of volcanic debris flows known as lahars. This model uses empirically derived, statistical descriptions of areas inundated by past mass-flow events to forecast areas likely to be inundated by hypothetical future events (sheet 3). Model coefficients can be adjusted to work with lahars/debris flows, rock avalanches, or materials with intermediate viscosities. The forecasts use power-law equations to relate a debris flow volume (V) to a cross-sectional inundation area (A) and a planimetric inundation area (B) via two equations:

$$(1)\ A = cV^{2/3}$$

$$(2)\ B = cV^{2/3}$$

The constant parameters (c) effectively define the viscosity of flowing material and dictate the resulting distribution of debris on the landscape. Materials can range from pure water to rock, with water being the least viscous and rock being the most viscous material. Water generates a narrow stream and travels a long distance, whereas rock debris forms a steep pile at the terminus of the debris flow. The behavior of a debris flow falls between the two extremes and depends on the material grain size, distribution of debris, and the roughness of the landscape. We use standard debris flow constants from Griswold and Iverson (2008) of 0.1 for cross-sectional area (in equation 1) and 20 for planimetric area (in equation 2).

The software is designed to automate equations (1) and (2) over a three-dimensional elevation model using (a) a starting point of debris accu-

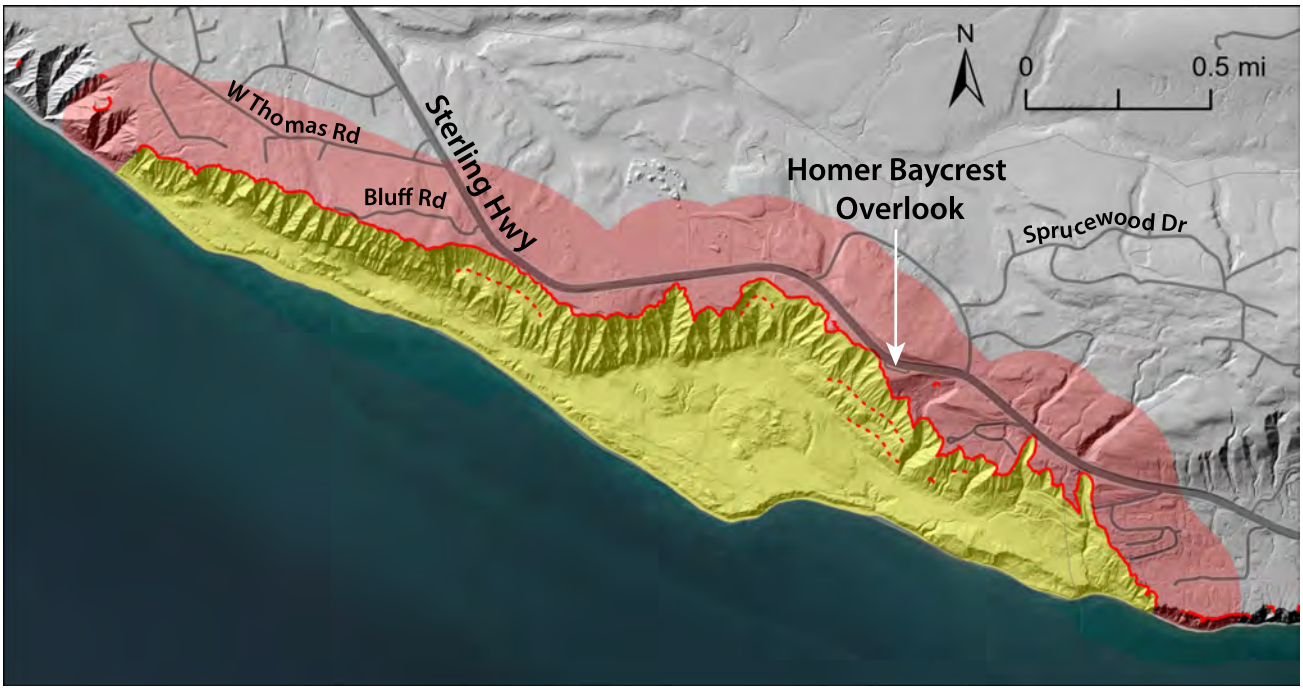

Figure 8. Deep-seated landslide susceptibility near the Bluff Point landslide (red polygon). The landslide body (yellow area, south of the red headscarp line) is the landslide deposit and is also susceptible to repeated failure.

mulation, (b) the total debris volume, and (c) the appropriate constant values described above. We chose the starting points of debris flows based on geomorphological evidence of debris accumulation within a catchment. This typically occurs at the transition from steep catchment slopes to flatter valley slopes, but it is dependent on the size, recent debris flow activity, and the degree of channelization within each catchment.

We simulate several debris volumes for each catchment. Assuming that earthflows mapped from aerial photographs and lidar data are shallow, or the approximate thickness of the mapped soil column (5 ft [1.42 m]), we calculate 5, 10, and 25 percent of the total volume of soil available in each catchment (fig. 9). For each catchment, we estimate the volume of landslides and earthflows identified in air photos and lidar and use this as an additional debris flow volume input (fig. 9). The maximum amount of topsoil in a catchment identified as having moved since 1952 is about 25 percent of the total catchment area; thus, we assume 25 percent of the total volume is an appropriate upper limit to the amount of sediment that might be available for mobilization in a saturated debris flow. However, one major assumption regarding potential sediment volumes is that none of the available sediment (from mapped earthflows) has already left the catchment via fluvial transport or channelized debris flows. The volumes we use are rough estimates of the potential available material. Of course, it is possible that 100 percent of the total soil volume in a catchment fails in a debris flow, but historical aerial photographs do not indicate that this has happened recently.

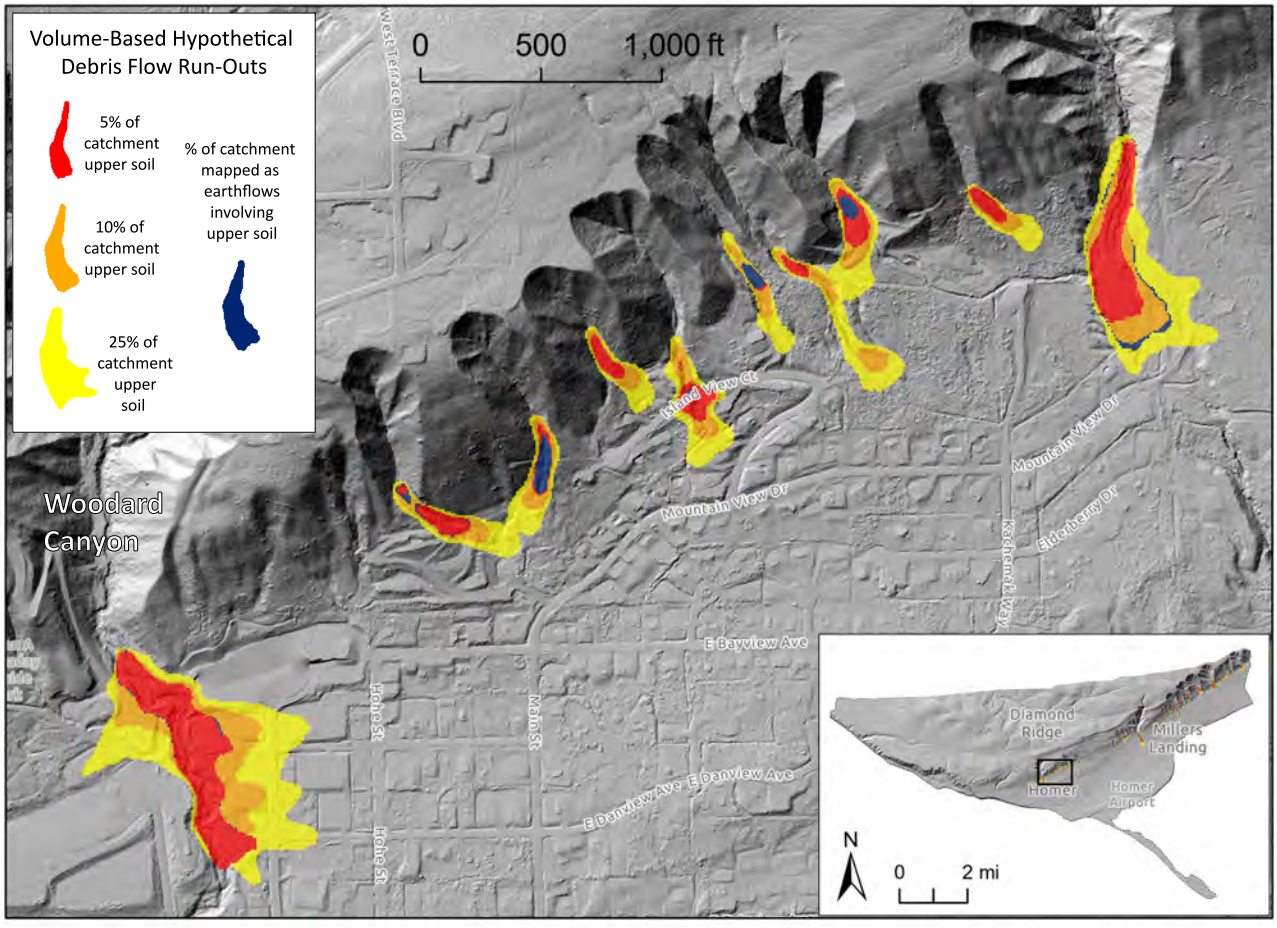

Figure 9. Excerpt from the Channelized Debris Flow runout map (map sheet 3). The percent of the Woodard Canyon catchment mapped as earthflows involving the upper soil column is just over five percent, and therefore, it is only barely visible between the red and the orange polygons.

Incremental volumes are calculated by cross-sectional area (perpendicular to flow direction), proceeding down the steepest path from the user-defined starting point. The distribution of material in a model result is based on the beginning position in a landscape, defined flow characteristics (model coefficient "c"), and initial volume. The model fills the lowest-lying areas in a cross section first (i.e., the active stream channel), spilling out onto the surrounding area (i.e., the alluvial fan) as dictated by the initial flow volume and local slope steepness. The model continues until the initial input volume is depleted. In some areas, the model produces unrealistic, spiky deposits because of small variations in the high-resolution bare earth elevation model. For all hypothetical runouts, we use ArcGIS Pro focal statistics and conditional tools to smooth the results.

RESULTS

Landslide Inventory and Database

Within the upland steep drainage catchments, we identified 678 slope failure scars in aerial photographs, including those present in the 1952 images. Nearly all these slope failures could be tied to geomorphological evidence (e.g., headscarps, over-steepened areas, slope failure deposits) in the 2019 lidar-derived elevation models. Table 3 summarizes the number and size distribution of photo-identified slope failures.

We identified an additional 404 slope failure scars using only the 2019 lidar data, many of which were along the coastline. We also identified 69 landslide deposits of various sizes throughout the study area. There is no additional event age data for these features. Most of these slope failure scars represent relatively small and shallow earthflows within the steep drainage catchments. Some notable exceptions include the channelized debris flows attributed to the 1964 earthquake and large topples from the face of the Bluff Point landslide headscarp (fig. 6). North of Kachemak City, at the end of China Poot Street, there is a significant, deep-seated paleo-landslide, the deposit of which covers 484,000 square feet (45,000 square meters) (figs. 5 and 6). This landslide is notable not only because of its size but also because the toe of the landslide deposit has been extensively excavated.

It should be noted that, except for the Bluff Point landslide headscarp, the coastline was not investigated using aerial photo sets. Nearly all the Homer and Kachemak City coastlines are susceptible to, or are currently undergoing, some sort of slope failure processes. Detailed coastline analysis and assessment of past and future trends is beyond the scope of this study but has been assessed in a parallel coastal bluff stability analysis (Buzard and Overbeck, 2022).

Factor of Safety Map

We calculated the FOS for the entire study area on a 5 m resampled bare earth elevation model (fig. 7; map sheet 2). Areas mapped as having elevated shallow landslide susceptibility are primarily on steep slopes. Our conservative anal-

Table 3. Summary of photo-identified slope failures.

Date	Number of slope failures	Average individual failure area ft² (m²)	Max individual failure area ft² (m²)	Sum total failure area ft² (m²)
prior to 1952	273	19,806 (1,840)	654,975 (60,013)	5,408,564 (502,472)
1952–1975	93	21,560 (2,003)	278,581 (25,881)	2,005,241 (186,293)
1975–mid 1980's	109	8,773 (815)	51,570 (4,791)	956,481 (88,860)
mid 1980's–2000	64	8,891 (826)	40,763 (3,787)	569,109 (52,872)
2000–2012/2013	60	3,832 (356)	14,908 (1,385)	230,380 (21,403)
2012/2013–2016	79	6,512 (605)	39,095 (3,632)	515,258 (47,869)

ysis (performed for soils at saturated conditions) suggests that slopes steeper than about 20–25 degrees are considered moderately susceptible to failure, and those steeper than about 30 degrees are highly susceptible to failure. The actively eroding canyon walls above Homer typically have steepnesses well into the highly susceptible category.

Deep-Seated Landslide Hazards

The Bluff Point landslide deposit (fig. 8, yellow area below the headscarp line) and the area immediately adjacent to and within 1,200 ft (430 m) of the Bluff Point landslide headscarp (fig. 8, red area above the headscarp line) present significant landslide hazards. Slope instability in the Bluff Point area is manifest as several different types of mass movements, each with varying severity. The most common type of failure occurs along the oversteepened inland Bluff Point headscarp or coastal bluffs as a mix of earthflows, rock falls, and cliff topples (fig 2). Natural or earthquake-induced fissures, as noted by Waller (1966) following the 1964 earthquake, make the cliffs more prone to toppling.

A more concerning type of instability involves deformation on new or reactivation of existing curved failure planes within the complex rotational landslide (fig. 2). In the case of Bluff Point, the toe of the original slide mass(es) extended into the ocean and was removed by coastal processes. Coupled with headscarp collapse onto the slide body, removal of the slide toe facilitates continued rotation—either as steady creep or in punctuated movements, the latter of which occurred in 2009 (Berg, 2009). In addition to an 820–1,000-foot-wide (250–300-m-wide) bluff collapse (identifiable in 2019 lidar, fig. 6), a several hundred-meter-wide stretch of the intertidal zone uplifted as much as 15 ft (~4.5 m) approximately 50–100 yards out in front of the main inland bluff (Berg, 2009). Progressive backtilting of sedimentary layers in the young slide block confirms deformation along a curved failure plane at depth. Ongoing coastal erosion and continued degradation of the Bluff Point headscarp wall (particularly as exacerbated by 1964-type earthquakes, extreme rainfall events, or uncharacteristically wet seasons driven by climate change) will drive continued slip on old failure planes and could eventually lead to reactivation of greater portions of the extensive landslide. Figure 8 highlights the area north of the Bluff Point headscarp that is potentially susceptible to continued deep-seated landslide failure. Particular attention should be paid to the western end of the Bluff Point landslide, where slopes are taller, steeper, more active, and poorly buttressed compared to the eastern half of the paleo-landslide.

The deep-seated paleo-landslide at the end of China Poot Street (figs. 5 and 6) also represents an area of elevated landslide hazard. The headscarp of the China Poot Street slide is approximately 130 ft (40 m) tall, so an appropriate horizontal buffer is about 260 ft (80 m) upslope of the primary headscarp. However, there is nothing developed immediately upslope of this landslide headscarp, so we do not explicitly draw the buffer. Development within and on the landslide deposit, and development in the mouths of catchments on either side of the China Poot Street landslide, should be considered to be at higher risk.

Additionally, in Thurston Canyon, just east of the 2019 lidar coverage, there is evidence of a deep-seated paleo-landslide on the northeast wall of the catchment (fig. 10). The established drainage in the main axis of the catchment and the incision of the landslide deposit itself suggest that it is relatively stable, but the original, oversteepened headwall has hosted small-scale earthflows as seen in neighboring catchments. This Thurston Canyon landslide is a good example of how a major, deep-seated failure within an upland catchment could either: 1) temporarily block exit flow from the catchment, eventually contributing to alluvial fan growth downstream in the form of repeat channelized debris flows; or 2) send deep-seated landslide debris directly out of the catchment as the landslide block disintegrates and flows downhill.

Debris Flow Runout Map

We simulated debris flow runouts for 47 individual catchments in Homer and Kachemak City (map sheet 3). For each catchment, we calculate flow volumes of 5, 10, and 25 percent of the estimated total soil volume, and where earthflows were identified in aerial photographs, the total volume of the identified earthflows in each catchment assumes a 5 ft (1.5 m) failure depth (fig. 9).

DISCUSSION AND LIMITATIONS

We developed the landslide inventory, shallow landslide susceptibility, deep landslide susceptibility, and debris flow runout maps using the best available data; however, there are many inherent limitations. The intended use of these overview maps is to help identify slopes with a relatively high slope failure hazard in and around Homer, to provide a basis for regional planning and increased resiliency, and to help identify localities where more detailed landslide mapping is warranted if areas are to be developed or improved. Limitations of the input data and modeling methods are such that the maps are not suitable to answer site-specific or legal questions. The maps should be used only for regional- or community-scale purposes.

The lidar-based mapping is a "snapshot" view of the current landscape based on available data and may change as new information regarding landslides becomes available and new landslides occur. Because we lack detailed site-specific information on every landslide, any existing engineered mitigative steps have not been accounted for. Local conditions may vary substantially from the parameters used to make these maps. It is likely that some slope failures were missed or misinterpreted by the map author, even using high-quality lidar-derived topographic data. We targeted our lidar survey point density to account for high vegetation density and known problem (i.e., unstable) areas, but we were only able to spot-check a few locations on the road system as part of this project.

The FOS calculations are sensitive to variability in the input parameters, and the map results are influenced by the accuracy and resolution of the input data for material properties, depth to failure, depth to groundwater, and slope angle. We estimated material properties based on available soils data, a limited amount of published field data, and

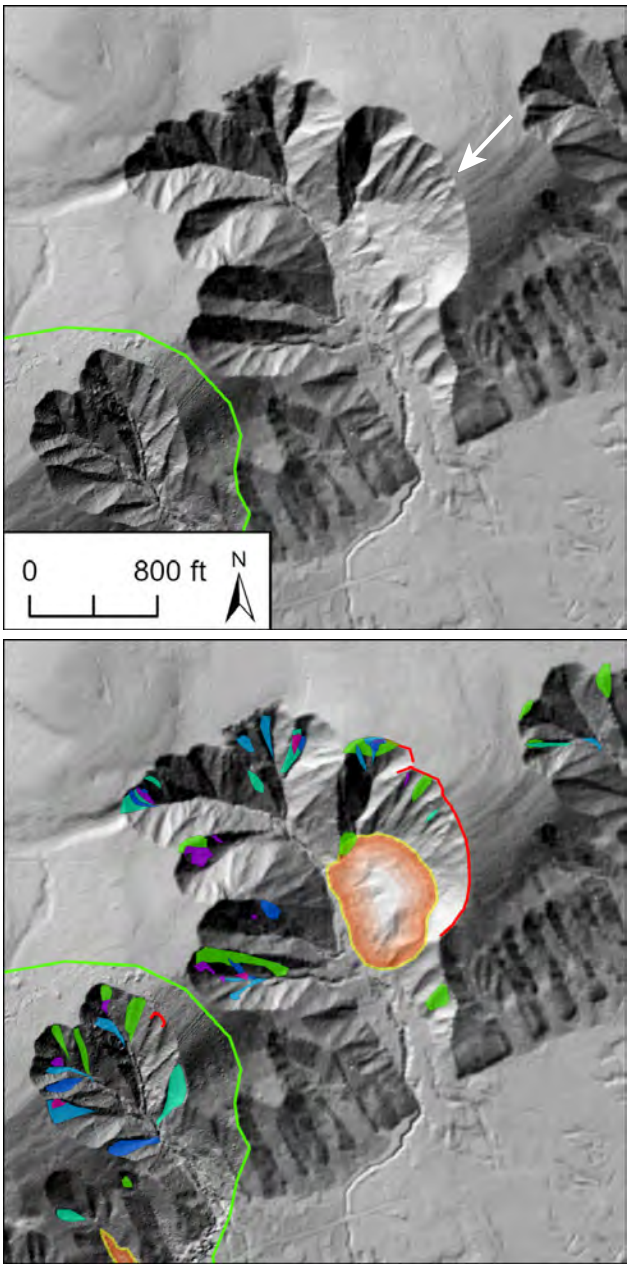

Figure 10. Deep-seated paleo-landslide on the east flank of Thurston Canyon, immediately east of the 2019 lidar coverage (2019 lidar extent delineated by green line). See figure 6 for symbol explanation.

assumed worst-case conditions. While it is possible for earthquakes to trigger slope failures, in a practical sense, the worst-case conditions mentioned here (i.e., saturated soils) will most likely be achieved through heavy seasonal precipitation or rain-on-snow events. Climate change is contributing to more variable weather patterns, from a changing snowpack to increased instances of extreme precipitation, and monitoring soil moisture conditions may be an important tool for monitoring evolving hazards.

Site-specific studies should be undertaken before development on existing landslide and debris flow deposits. Many of the drainages in Homer's steep catchments are conduits for debris, and many catchments have debris flow fans at their bases, indicating that several debris flows have occurred there in the past. At some sites, excavated debris flows are more than 40 ft (~12 m) thick and are comprised of many individual debris flows. We recommend site-specific investigations by qualified geotechnical engineers to evaluate recent activity of debris flow fans and to test subsurface soil conditions for suitability in construction projects.

Debris flow runout modeling is primarily based on estimates of the sediment volume for each catchment and the point at which slope failures will begin deposition of materials. Although these estimates are based on our best assessment of the data, many factors can lead to large differences in the estimates and actual landslide runouts. For example, interaction of a debris flow with buildings or engineered earth materials can change the direction of flow. Large trees or other objects in a debris flow can change the final runout length and width. Lastly, the lidar-based digital elevation model contains artifacts from the removal of man-made structures (e.g., homes, porches). It would require extensive GIS and field work to locate and remove all structures completely.

Although several landslides were mapped by Waller (1966) after the 1964 Great Alaska Earthquake, anecdotal evidence and air photo analyses indicate that there were potentially many more landslides in Homer. Several additional photo-identified channelized debris flows occurred between 1952 and 1975 that were not mapped by Waller (1966) but exhibit similar characteristics to those that occurred during the 1964 event (e.g., fig. 4C, channelized debris flow in Neilsen Canyon). We did not identify other channelized debris flows in aerial photographs taken since 1952, and those that occurred in 1964 cover significantly more area (at ~23,000 square meters and ~25,000 square meters each) than most other slope failures since 1952. Furthermore, it is likely that there was significantly more fissuring at the tops of bluffs and along the deep-seated paleo-landslide scarps than was observed by Waller (1966). This is reasonable, given that at that time, far less of Homer was developed and access was significantly limited compared to today. With respect to potential earthquake-induced ground failures, Waller (1966) notes that "landslide hazards exist…anywhere that promontories extend out from precipitous bluffs and cliffs." Analysis of potential compound hazards—such as soil liquefaction on slopes—is beyond the scope of this project.

Lastly, evidence from Thurston Canyon and elsewhere along the shores of Kachemak Bay suggests that there is potential for large volume, deep-seated landslides in the upland catchments to disintegrate and flow downhill into developed areas. Modeling these types of failures and runouts would be purely speculative, but we cannot rule out the possibility that such an event may occur.

CONCLUSION

DGGS completed a comprehensive landslide hazard assessment for the City of Homer by creating a map and database of historical and prehistoric slope failures, maps of shallow and deep-seated landslide susceptibility, and a map of simulated debris flow runouts for the City of Homer and neighboring Kachemak City. Data from these analyses are collectively intended to depict overall landslide hazard, and the results provide important information that can help guide planning and future investigations. The maps are not intended

to predict slope failures, and site-specific, detailed investigations should be conducted prior to development in vulnerable areas. Results are for informational purposes and may not be used for legal, engineering, or surveying uses.

ACKNOWLEDGMENTS

DGGS collected and processed lidar for use in this landslide hazard resiliency project for the City of Homer, funded by the Federal Emergency Management Agency (FEMA) through Cooperating Technical Partnership (CTP) with the City of Homer and DGGS under federal grant number CTP EMS-2018-CA-00016-S01. DGGS thanks the Homer Planning Commission for guidance throughout the multi-year project, and Jonathan Godt, Rich Buzard, and Bretwood Higman for constructive reviews that greatly improved this manuscript.

REFERENCES

Alaska Department of Commerce, Community, and Economic Development, 2017, Kenai Peninsula Risk Report: Federal Emergency Management Agency Risk Report, 89 p. https://www.commerce.alaska.gov/web/Portals/4/pub/risk_report_kenai_final.pdf

Barnes, F.F., and Cobb, E.H., 1959, Geology and coal resources of the Homer District, Kenai coal field, Alaska: U.S. Geological Survey Bulletin 1085-F, p. 203–208.

Berg, Ed, 2009, Sudden uplift of the beach recalls ancient landslides, *in* Berg, Ed, ed., Refuge Notebook: U.S. Fish & Wildlife Service Kenai National Wildlife Refuge Notebook, v. 11, no. 27, p. 54–55. https://ecos.fws.gov/ServCat/Reference/Profile/128174

Berg, Ed, Reger, Dick, and Higman, Bretwood, 2014, Geologists determine age of Bluff Point Landslide, *in* Morton, J.M., ed., Refuge Notebook: U.S. Fish & Wildlife Service Kenai National Wildlife Refuge Notebook, v. 16, no. 32, p. 63–64. https://ecos.fws.gov/ServCat/Reference/Profile/128179

Burns W.J., and Madin I.P., 2009, Protocol for inventory mapping of landslide deposits from light detection and ranging (lidar) imagery: Oregon Department of Geology and Mineral Industries Special Paper 42, 30 p. https://www.oregongeology.org/pubs/sp/p-SP-42.htm

Burns W.J., Madin I.P., and Mickelson, K.A., 2012, Protocol for shallow landslide susceptibility mapping: Oregon Department of Geology and Mineral Industries Special Paper 45, 32 p. https://www.oregongeology.org/pubs/sp/p-SP-45.htm

Burns, W.J., and Mickelson, K.A., 2016, Protocol for deep landslide susceptibility mapping: Oregon Department of Geology and Mineral Industries Special Paper 48, 66 p. https://www.oregongeology.org/pubs/sp/p-SP-48.htm

Buzard, R.M., and Overbeck, J.R., 2022, Coastal bluff stability assessment for Homer, Alaska: Alaska Division of Geological & Geophysical Surveys Report of Investigation 2022-5, 22 p., 2 sheets, scale 1:50,000. https://doi.org/10.14509/30908

Carver, G.A., and Plafker, George, 2008, Paleoseismicity and neotectonics of the Aleutian subduction zone—An overview, *in* Freymueller, J.T., Haeussler, P.J., Wesson, R.L, and Ekström, G., eds., Active tectonics and seismic potential of Alaska: American Geophysical Union Monograph 179, p. 43–63.

Cruden, D.M., and Varnes, D.J., 1996, Landslide types and processes, *in* Turner, A.K., and Schuster, R.L., eds., Landslides—Investigation and mitigation: Transportation Research Board, Special report no. 247, National Academy of Sciences, Washington, D.C., p. 36–75.

Cornforth, D.H., 2005, Landslides in practice: Investigation, analysis, and remedial/preventative options in soils: Hoboken, N.J., John Wiley and Sons, 596 p.

Griswold, J.P., and Iverson, R.M., 2008, Mobility statistics and automated hazard mapping for debris flows and rock avalanches: U.S. Geological Survey Scientific Investigations Report 2007-5276, 59 p.

Highland, L.M., and Bobrowsky, Peter, 2008, The landslide handbook—A guide to understanding landslides: Reston, Virginia, U.S. Geological Survey Circular 1325, 129 p.

Highland, L.M., and Johnson, Margo, 2004, Landslide types and processes: U.S. Geological

Survey Fact Sheet 2004-3072, 4 p. https://pubs.usgs.gov/fs/2004/3072/pdf/fs2004-3072.pdf

Hubbard, T.D., Daanen, R.P., and Stevens, D.S.P., 2024, Debris flow hazard evaluations for multi-hazard risk mapping in Sitka, Alaska: Alaska Division of Geological & Geophysical Surveys Report of Investigation 2024-2, 13 p., 6 sheets. https://doi.org/10.14509/30187

Jakob, Matthias, 2005, A size classification for debris flows: Engineering Geology, v. 79, p. 151–161.

Keefer, D.K., and Johnson, A.M., 1983, Earth flows; morphology, mobilization, and movement: U.S. Geological Survey Professional Paper 1264, 53 p. https://doi.org/10.3133/pp1264

Nishenko, S.P., 1991, Circum-Pacific seismic potential, 1989–1999: Pure and Applied Geophysics, v. 135, no. 2, p. 169–259. http://doi.org/10.1007/BF00880240

Nishenko, S.P., and Jacob, K.H., 1990, Seismic potential of the Queen Charlotte–Alaska–Aleutian seismic zone: Journal of Geophysical Research, v. 95, no. B3, p. 2,511–2,532. http://doi.org/10.1029/JB095iB03p02511

Plafker, George, 1969, Tectonics of the March 27, 1964, Alaska earthquake: U.S. Geological Survey Professional Paper 543-I, p. I1–I74, 2 sheets.

Reger, R.D., 1978, Bluff Point landslide, a massive ancient rock failure near Homer, Alaska: Alaska Division of Geological & Geophysical Surveys Short Notes on Alaskan Geology, Geologic Report 61 B, p. 5–9. https://doi.org/1014509/409

Reger, R.D., Sturmann, A.G., Berg, E.E., and Burns, P.A.C., 2007, A guide to the late Quaternary history of northern and western Kenai Peninsula, Alaska: Alaska Division of Geological & Geophysical Surveys Guidebook 8, 112 p., 6 sheets, scale 1:63,360. http://doi.org/10.14509/15941

Salisbury, J.B., Herbst, Andrew, and Daanen, R.P., 2021, High-resolution lidar data for Homer, Alaska: Division of Geological & Geophysical Surveys Raw Data File 2021-2, 6 p. https://doi.org/10.14509/30591

Schilling, S.P., 1998, LAHARZ: GIS programs for automated mapping of lahar-inundation hazard zones: U.S. Geological Survey Open-File Report 98-638, 80 p. https://pubs.usgs.gov/of/1998/0638/report.pdf

Shennan, Ian, and Hamilton, Sarah, 2006, Coseismic and pre-seismic subsidence associated with great earthquakes in Alaska: Quaternary Science Reviews, v. 25, 8 p. https://doi.org/10.1016/j.quascirev.2005.09.002

Shennan, Ian, Barlow, Natasha, Carver, Gary, Davies, Frank, Garrett, Ed, and Hocking, Emma, 2014, Great tsunamigenic earthquakes during the past 1,000 yr on the Alaska megathrust: Geology, v. 42, no. 8, p. 687–690. http://doi.org/10.1130/G35797.1

United States Department of Agriculture Natural Resources Conservation Service (USDA NRCS), 2005, Soil Survey of Western Kenai Peninsula Area, Alaska, 618 p. https://websoilsurvey.nrcs.usda.gov/app/WebSoilSurvey.aspx

U.S. Geological Survey ShakeMap, M 9.2 – 1964 Prince William Sound Earthquake, Alaska, event ID 19640328033616_30. https://earthquake.usgs.gov/earthquakes/eventpage/official19640328033616_30/executive [accessed March, 2021]

Varnes, D.J., 1978, Slope movement types and processes, *in* Schuster, R.L., and Krizek, R.J., eds., Landslides analysis and control: Transportation Research Board Special Report 176, National Academy of Sciences, Washington, D.C., p. 11–33. http://onlinepubs.trb.org/Onlinepubs/sr/sr176/176.pdf

Waller, R.M.,1966, Effects of the earthquake of March 27, 1964 in the Homer Area, Alaska: U.S. Geological Survey Professional Paper 542-D, 28 p.

Wesson, R.L., Boyd, O.S., Mueller, C.S., Bufe, C.G., Frankel, A.D., and Petersen, M.D., 2007, Revision of time-Independent probabilistic seismic hazard maps for Alaska: U.S. Geological Survey Open-File Report 2007-1043, 33 p.

Wilson, F.H., and Hults, C.P., 2012, Geology of the Prince William Sound and Kenai Peninsula region, Alaska: U.S. Geological Survey Scientific Investigations Map 3110, 38 p., 1 sheet.

REPORT OF INVESTIGATION 2024-3
Salisbury, J.B., 2024
SHEET 1 OF 3
Explanatory report accompanies map
https://doi.org/10.14509/31155

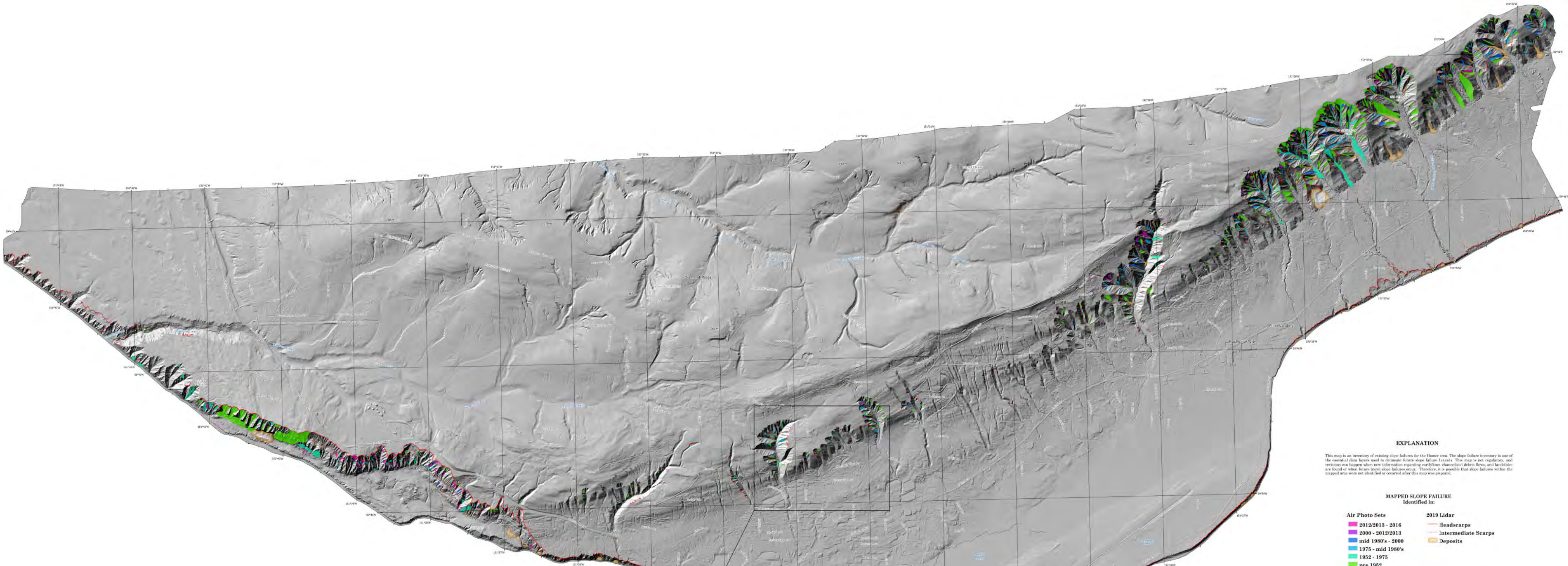

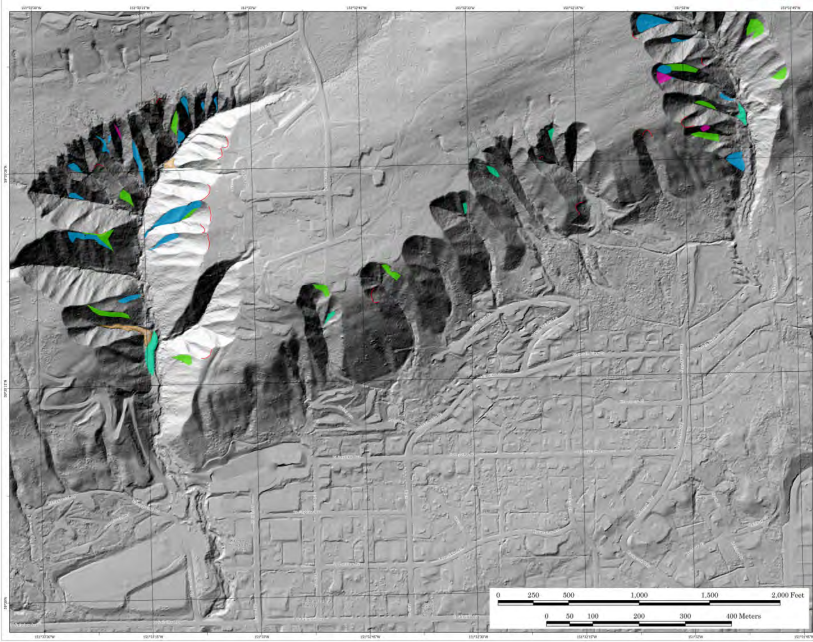

Slope Failure Inventory for Homer, Alaska

by
J.B. Salisbury

2024

SCALE: 1:13,500

0 0.25 0.5 0.75 1 Mile

0 1,000 2,000 3,000 4,000 Feet

0 0.5 1 1.5 2 Kilometers

EXPLANATION

This map is an inventory of existing slope failures for the Homer area. The slope failure inventory is one of the essential data layers used to delineate future slope failure hazards. This map is not regulatory, and revisions can happen when new information regarding earthflows channelized debris flows, and landslides are found or when future (new) slope failures occur. Therefore, it is possible that slope failures within the mapped area were not identified or occurred after this map was prepared.

MAPPED SLOPE FAILURE
Identified in:

Air Photo Sets
- 2012/2013 - 2016
- 2000 - 2012/2013
- mid 1980's - 2000
- 1975 - mid 1980's
- 1952 - 1975
- pre 1952

2019 Lidar
- Headscarps
- Intermediate Scarps
- Deposits

LIMITATIONS

This slope failure inventory map was developed with the best available data, using protocols similar to those of Burns and Madin (2009) and Burns and others (2012), however, there are inherent limitations as discussed below. These limitations underscore that this map is designed for regional application and should not be used as an alternative to site-specific studies.

While every effort was made to map all recent and prehistoric slope failures, given the limitations in available imagery, field validation, and the vegetation density, it is likely that some slope failures were missed, overlooked, or misinterpreted by the map authors, even with high-quality lidar-derived topographic data. The maps were reviewed to minimize these problems.

The lidar-based mapping is a "snapshot" view of the current landscape that may change as new information regarding slope failures becomes available, including the occurrence of new slope failures.

The map is intended to assist state and local agencies in land-use planning. The map cannot replace site-specific investigations and is not suitable for land-use regulation and building-code development. However, the map can serve as a useful tool for estimating the regional slope failure hazard and as a starting place for future site-specific maps.

ACKNOWLEDGEMENTS

DGGS collected and processed lidar for use in a landslide hazard resiliency project for the City of Homer, funded by the Federal Emergency Management Agency (FEMA) through Cooperating Technical Partnership (CTP) with the City of Homer and AK DGGS under federal grant number CTP EMS-2018-CA-00016-S01.

REFERENCES CITED

Burns W.J., and Madin I.P., 2009, Protocol for inventory mapping of landslide deposits from light detection and ranging (lidar) imagery: Oregon Department of Geology and Mineral Industries Special Paper 42, 30 p. https://www.oregongeology.org/pubs/sp/p-SP-42.htm

Burns W.J., Madin I.P., and Mickelson, K.A., 2012, Protocol for shallow landslide susceptibility mapping: Oregon Department of Geology and Mineral Industries Special Paper 45, 32 p. https://www.oregongeology.org/pubs/sp/p-SP-45.htm

Salisbury, J.B., Daanen, R.P., and Herbst, A.M., 2021, Lidar-derived elevation models for Homer, Alaska: Alaska Division of Geological and Geophysical Surveys Raw Data File 2021-2, 6 p. https://doi.org/10.14509/30591

STATE OF ALASKA
DEPARTMENT OF NATURAL RESOURCES
DIVISION OF GEOLOGICAL & GEOPHYSICAL SURVEYS
3354 College Road ♦ Fairbanks, Alaska 99709-3707
Phone 907-451-5010 ♦ Fax 907-451-5050
email: dggspubs@alaska.gov ♦ website: dggs.alaska.gov

This project was funded by the FEMA Cooperating Technical Partners Program (grant number EMS-2018-CA-00016-S01).

Base Map: Lidar-derived hillshade image from Salisbury and others, 2021.
Lidar Data Reviewed by: FEMA Staff

Reference Layer Sources: Esri, HERE, Garmin, FAO, NOAA, USGS, OpenStreetMap contributors, and the GIS User Community

Data and Map Coordinate System: NAD 1983 (2011) UTM Zone 5N, vertical datum NAVD88 with GEOID12B correction for Alaska

Software: ArcGIS Pro 3.2.2

Cartography by: J.B. Salisbury
Cartographic review by: A.E. MacPherson

REPORT OF INVESTIGATION 2024-3
Salisbury, J.B., 2024
SHEET 2 OF 3
Explanatory report accompanies map
https://doi.org/10.14509/31155

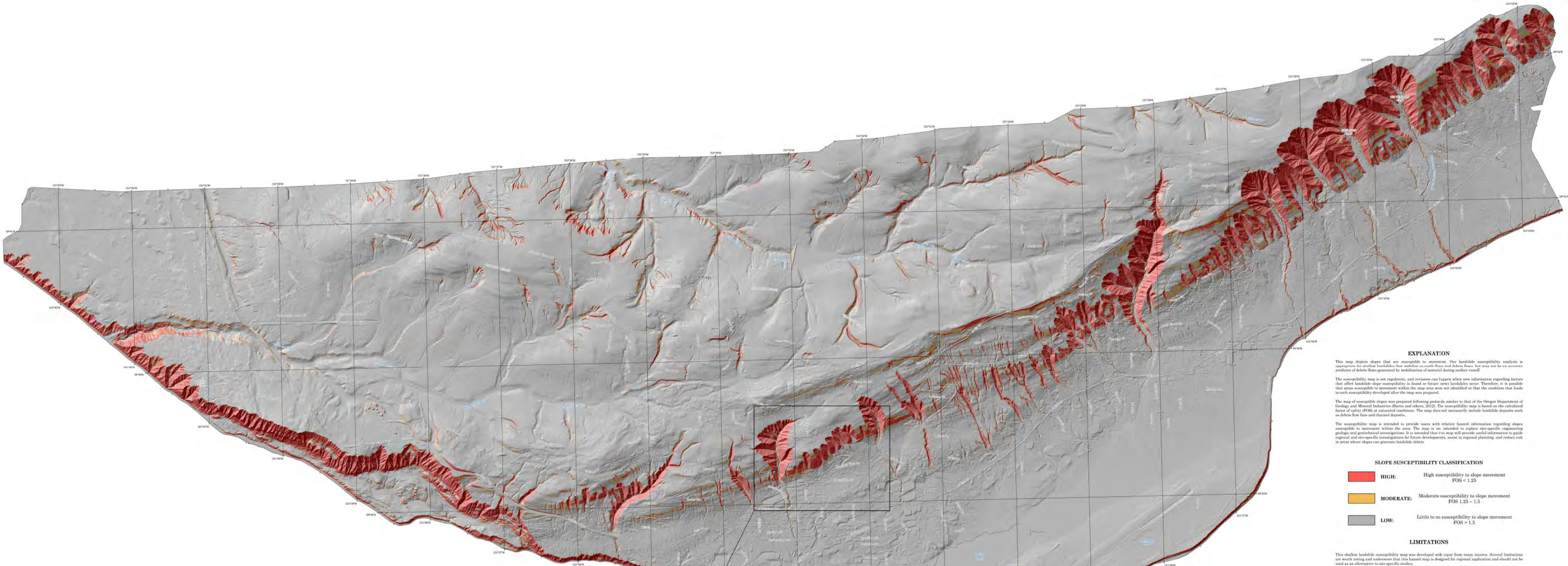

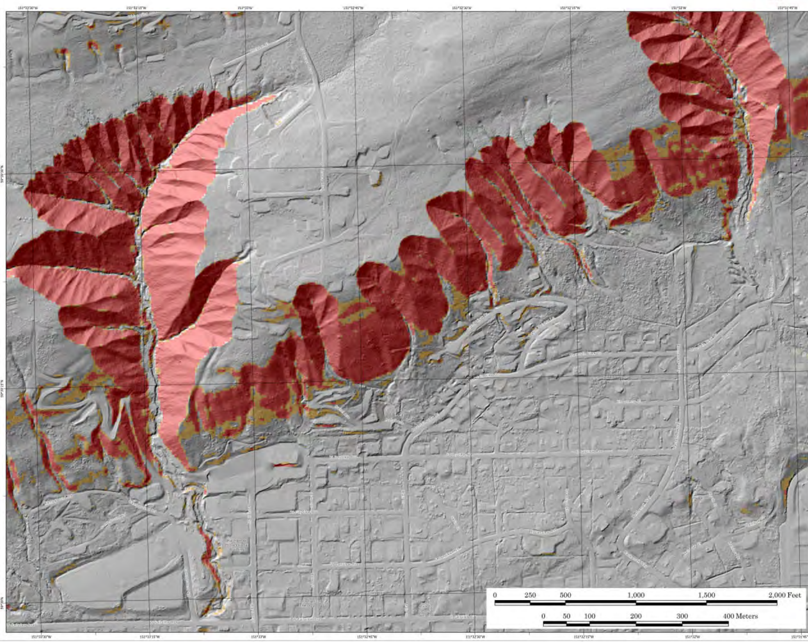

Shallow Landslide Susceptibility for Homer, Alaska

by

J.B. Salisbury

2024

SCALE: 1:13,500

0 0.25 0.5 0.75 1 Mile

0 1,000 2,000 3,000 4,000 Feet

0 0.5 1 1.5 2 Kilometers

EXPLANATION

This map depicts slopes that are susceptible to movement. Our landslide susceptibility analysis is appropriate for shallow landslides that mobilize as earth flows and debris flows, but may not be an accurate predictor of debris flows generated by mobilization of material during surface runoff.

The susceptibility map is not regulatory, and revisions can happen when new information regarding factors that affect landslide slope susceptibility is found or future (new) landslides occur. Therefore, it is possible that areas susceptible to movement within the map area were not identified or that the condition that leads to such susceptibility developed after the map was prepared.

The map of susceptible slopes was prepared following protocols similar to that of the Oregon Department of Geology and Mineral Industries (Burns and others, 2012). The susceptibility map is based on the calculated factor of safety (FOS) at saturated conditions. The map does not necessarily include landslide deposits such as debris flow fans and channel deposits.

The susceptibility map is intended to provide users with relative hazard information regarding slopes susceptible to movement within the area. The map is not intended to replace site-specific engineering geologic and geotechnical investigations. It is intended that this map will provide useful information to guide regional and site-specific investigations for future developments, assist in regional planning, and reduce risk in areas where slopes can generate landslide debris.

SLOPE SUSCEPTIBILITY CLASSIFICATION

(red)	**HIGH:**	High susceptibility to slope movement FOS < 1.25
(orange)	**MODERATE:**	Moderate susceptibility to slope movement FOS 1.25 – 1.5
(gray)	**LOW:**	Little to no susceptibility to slope movement FOS > 1.5

LIMITATIONS

This shallow landslide susceptibility map was developed with input from many sources. Several limitations are worth noting and underscore that this hazard map is designed for regional application and should not be used as an alternative to site-specific studies.

This map is based on a calculated factor of safety (FOS). Factors that can affect the level of detail and accuracy of the final susceptibility map include:

a. The infinite slope factor of safety calculations are done on one individual grid cell at a time without regard for the adjacent grid cells. We calculate FOS at ~15 ft (5 m) resolution to reduce local overestimation in areas of steep slopes with low relief; however, some local estimation is still possible.

b. The FOS calculations are strongly influenced by the accuracy and resolution of the input data for material properties, depth to failure, depth to groundwater, and slope steepness. Material properties are estimated based on soils data from the U.S. Department of Agriculture (USDA, 2005) and are conservative estimates. Slope steepness is based on remotely-sensed lidar data at ~15 ft (5 m) resolution (Salisbury and others, 2021).

c. Local conditions may vary substantially from the values used to make this map.

The susceptibility map is based on topographic data available as of the date of publication.

The lidar-based digital elevation model has been edited to remove man-made structures, though many artifacts remain in the data (Salisbury and others, 2021).

The map is intended for regional purposes only and is intended to assist state and local agencies in land-use planning. The map cannot replace site-specific investigations and is not suitable for land-use regulation and building-code development. However, the map can serve as a useful tool for estimating the regional shallow landslide hazard and as a starting place for future site-specific investigations.

ACKNOWLEDGEMENTS

DGGS collected and processed lidar for use in a landslide hazard resiliency project for the City of Homer, funded by the Federal Emergency Management Agency (FEMA) through Cooperating Technical Partnership (CTP) with the City of Homer and AK DGGS under federal grant number CTP EMS-2018-CA-00016-S01.

REFERENCES CITED

Burns W.J., Madin I.P., and Mickelson, K.A., 2012, Protocol for shallow landslide susceptibility mapping: Oregon Department of Geology and Mineral Industries Special Paper 45, 32 p. https://www.oregongeology.org/pubs/sp/p-SP-45.htm

United States Department of Agriculture (USDA), 2005, Natural Resources Conservation Service Soil Survey of Western Kenai Peninsula Area, Alaska, 618 p., accessed via Web Soil Survey compiled in 2018. https://websoilsurvey.nrcs.usda.gov/app/WebSoilSurvey.aspx

Salisbury, J.B., Daanen, R.P., and Herbst, A.M., 2021, Lidar-derived elevation models for Homer, Alaska: Alaska Division of Geological and Geophysical Surveys Raw Data File 2021-2, 6 p. https://doi.org/10.14509/30591

STATE OF ALASKA
DEPARTMENT OF NATURAL RESOURCES
DIVISION OF GEOLOGICAL & GEOPHYSICAL SURVEYS
3354 College Road ♦ Fairbanks, Alaska 99709-3707
Phone 907-451-5010 ♦ Fax 907-451-5050
email: dggspubs@alaska.gov ♦ website: dggs.alaska.gov

This project was funded by the FEMA Cooperating Technical Partners Program (grant number EMS-2018-CA-00016-S01).

Base Map: Lidar-derived hillshade image from Salisbury and others, 2021.
Lidar Data Reviewed by: FEMA Staff

Reference Layer Sources: Esri, HERE, Garmin, FAO, NOAA, USGS, OpenStreetMap contributors, and the GIS User Community

Data and Map Coordinate System: NAD 1983 (2011) UTM Zone 5N, vertical datum NAVD88 with GEOID12B correction for Alaska

Software: ArcGIS Pro 3.2.2

Cartography by: J.B. Salisbury
Cartographic review by: A.E. MacPherson

REPORT OF INVESTIGATION 2024-3
Salisbury, J.B., 2024
SHEET 3 OF 3
Explanatory report accompanies map
https://doi.org/10.14509/31155

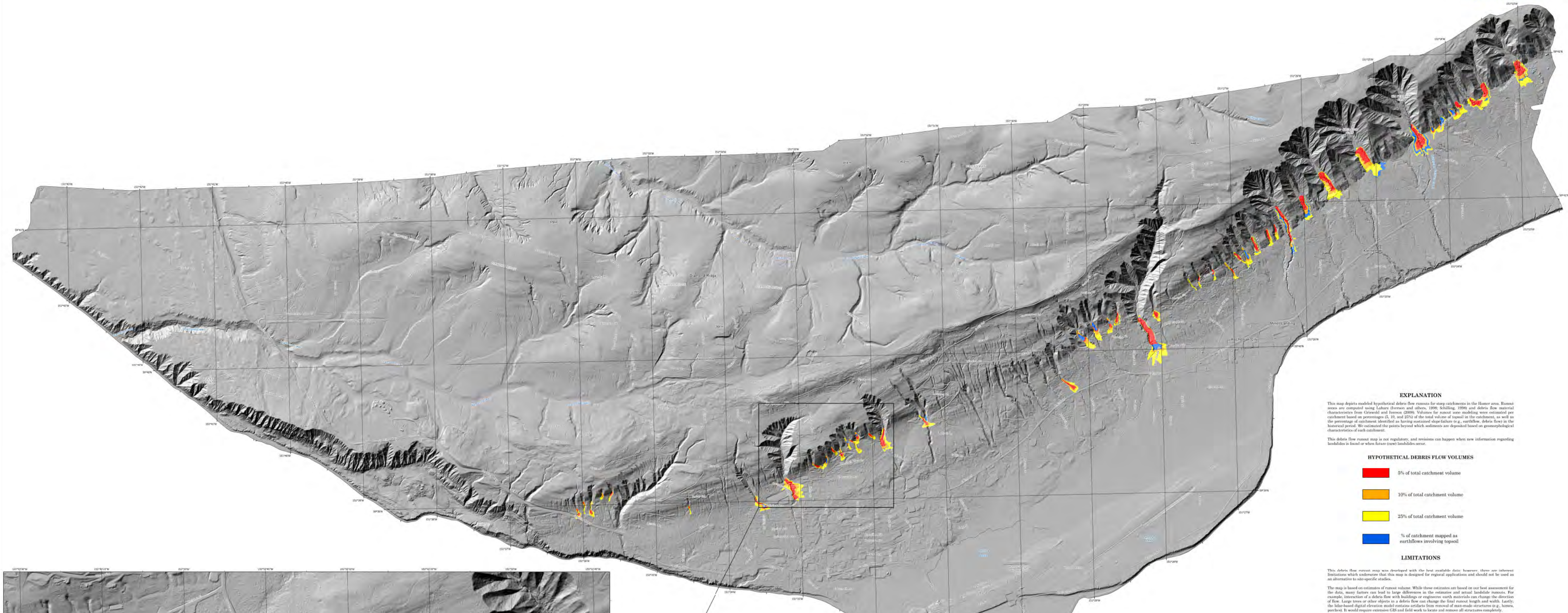

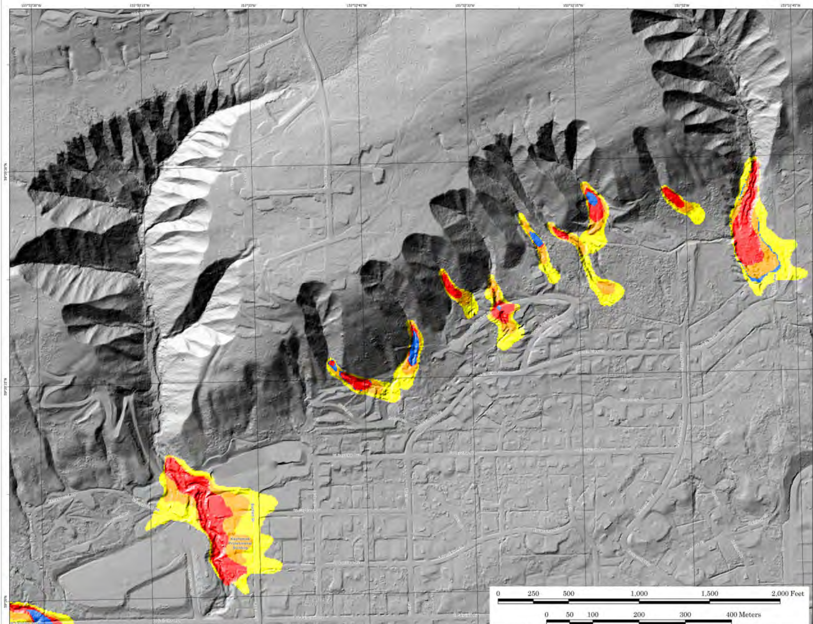

EXPLANATION

This map depicts modeled hypothetical debris flow runouts for steep catchments in the Homer area. Runout zones are computed using Laharz (Iverson and others, 1998; Schilling, 1998) and debris flow material characteristics from Griswold and Iverson (2008). Volumes for runout zone modeling were estimated per catchment based on percentages (5, 10, and 25%) of the total volume of topsoil in the catchment, as well as the percentage of catchment identified as having sustained slope failure (e.g., earthflow, debris flow) in the historical period. We estimated the points beyond which sediments are deposited based on geomorphological characteristics of each catchment.

This debris flow runout map is not regulatory, and revisions can happen when new information regarding landslides is found or when future (new) landslides occur.

HYPOTHETICAL DEBRIS FLOW VOLUMES

5% of total catchment volume

10% of total catchment volume

25% of total catchment volume

% of catchment mapped as earthflows involving topsoil

LIMITATIONS

This debris flow runout map was developed with the best available data; however, there are inherent limitations which underscore that this map is designed for regional applications and should not be used as an alternative to site-specific studies.

The map is based on estimates of runout volume. While these estimates are based on our best assessment for the data, many factors can lead to large differences in the estimates and actual landslide runouts. For example, interaction of a debris flow with buildings or engineered earth materials can change the direction of flow. Large trees or other objects in a debris flow can change the final runout length and width. Lastly, the lidar-based digital elevation model contains artifacts from removal of man-made structures (e.g., homes, porches). It would require extensive GIS and field work to locate and remove all structures completely.

The map is intended for regional purposes only and is intended to assist state and local agencies in land-use planning. The map cannot replace site-specific investigations and is not suitable for land-use regulation and building-code development. However, the map can serve as a useful tool for estimating the regional landslide runout hazard and as a starting place for future site-specific maps.

ACKNOWLEDGEMENTS

DGGS collected and processed lidar for use in a landslide hazard resiliency project for the City of Homer, funded by the Federal Emergency Management Agency (FEMA) through Cooperating Technical Partnership (CTP) with the City of Homer and AK DGGS under federal grant number CTP EMS-2018-CA-00016-S01.

REFERENCES CITED

Griswold, J.P., and Iverson, R.M., 2008, Mobility statistics and automated hazard mapping for debris flows and rock avalanches: U.S. Geological Survey Scientific Investigations Report 2007-5276, 59 p.

Iverson, R.M., Schilling, S.P., and Vallance, J.W., 1998, Objective delineation of lahar-inundation hazard zones: GSA Bulletin, v. 110, no. 8, p. 972 – 984. https://pubs.geoscienceworld.org/gsa/gsabulletin/article-pdf/110/8/972/3383034/i0016-7606-110-8-972.pdf

Salisbury, J.B., Daanen, R.P., and Herbst, A.M., 2021, Lidar-derived elevation models for Homer, Alaska: Alaska Division of Geological and Geophysical Surveys Raw Data File 2021-2, 6 p. https://doi.org/10.14509/30591

Schilling, S.P., 1998, LAHARZ: GIS programs for automated mapping of lahar-inundation hazard zones: U.S. Geological Survey Open-File Report 98-638, 80 p. https://pubs.usgs.gov/of/1998/0638/report.pdf

Modeled Debris Flow Runouts for Homer, Alaska

by
J.B. Salisbury

2024

SCALE: 1:13,500

0 0.25 0.5 0.75 1 Mile

0 1,000 2,000 3,000 4,000 Feet

0 0.5 1 1.5 2 Kilometers

STATE OF ALASKA
DEPARTMENT OF NATURAL RESOURCES
DIVISION OF GEOLOGICAL & GEOPHYSICAL SURVEYS
3354 College Road ♦ Fairbanks, Alaska 99709-3707
Phone 907-451-5010 ♦ Fax 907-451-5050
email: dggspubs@alaska.gov ♦ website: dggs.alaska.gov

This project was funded by the FEMA Cooperating Technical Partners Program (grant number EMS-2018-CA-00016-S01).

Base Map: Lidar-derived hillshade image from Salisbury and others, 2021.
Lidar Data Reviewed by: FEMA Staff

Reference Layer Sources: Esri, HERE, Garmin, FAO, NOAA, USGS, OpenStreetMap contributors, and the GIS User Community

Data and Map Coordinate System: NAD 1983 (2011) UTM Zone 5N, vertical datum NAVD88 with GEOID12B correction for Alaska

Software: ArcGIS Pro 3.2.2

Cartography by: J.B. Salisbury
Cartographic review by: A.E. MacPherson

Carla Stanley, representing the City of Homer

Update from the Board of Directors

Cook Inlet Regional Citizens Advisory Council

The Cook Inlet Regional Citizens Advisory Council held its regular meeting December 5th and 6th in Anchorage.

During the first day of meetings, the Council approved the special election of Brent Johnson. Mr. Johnson will represent the Commercial Fishing group on the Board. He brings more than 50 years of knowledge and experience in the local fishing community and has served on the Kenai Peninsula Borough Assembly since 2014 and currently serves as Assembly President. We are excited to welcome him to the Council.

On Friday, the Council received updates from several of its Ex-Officio members, including the US Coast Guard. Captain Christopher Culpepper, Commanding Officer Sector Western Alaska and US Arctic, explained some changes coming to USCG stations in Homer and Seward. Current-generation Cutters stationed there will be decommissioned and replaced with newer, 154-foot vessels along with larger crews. Those staffing changes are expected to happen early next year.

Givey Kochanowski, Alaska Regional Director for the Bureau of Ocean Energy Management (BOEM) spoke to the Council about the Bureau's environment program, intended to provide decision makers with the appropriate science to ensure offshore energy production happens safely and responsibly. He noted new studies and pilot projects within the National Energy Laboratory focused on renewable sources, such as wind, tidal, and wave, all of which have potential in Cook Inlet. Those programs focus on integrating marine and social sciences, biology, and traditional knowledge.

Cook Inlet Spill Prevention and Response, Inc. (CISPRI) General Manager Todd Paxton gave an update on his organization's plans for potentially replacing one of its primary response vessels, the Perseverance. That 207-foot ship, built in 1976, could be replaced by a new or repurposed vessel. CISPRI has also recently updated its registration as a primary contractor to provide Oil Spill Response Organization (OSRO) services beyond Cook Inlet.

The Council also heard reports from the National Oceanic and Atmospheric Administration (NOAA). Alaska Sea Ice Coordinator Michael Lawson gave an overview of the Cook Inlet Ice Camera Network, and how it's deployed in forecasting models and its importance in observation and data-gathering. CIRCAC staff developed the idea for and established the network nearly 20 years ago. One of the many planning and response improvements adopted after the grounding of the Seabulk Pride in 2006 was to provide real-time views of ice conditions. The network now includes nine cameras positioned at strategic points from the mouth of the Kenai River to the Don Young Port of Alaska. NOAA's Alaska Regional Preparedness Coordinator and Scientific Support Coordinator for the Alaska Regional Response Team, Liza Sanden made the Council aware of new virtual training opportunities for Shoreline Cleanup and Assessment Techniques (SCAT) coming up in the Spring.

Steve Ribuffo, Port Director for the Don Young Port of Alaska in Anchorage updated the Council on the facility's Petroleum and Cement Terminal construction. Completed in 2022, that terminal represents part of a long term modernization plan that is being completed in phases. In 2025, work will continue on Phase II – North Extension Stabilization, which will expand the port's capacity in the future. Other work will include demolition and replacement of cargo terminals and a second North Extension Stabilization project.

The Council also heard an operations update from Captain Jeff Brue, Global Marine Operations Manager for Marathon Petroleum.

The Council will hold its Annual Meeting on April 4th in Kenai.